

Air quality impacts of electricity purchase and air travel by organizations

Yuang Chen¹, Florian Allrogen², Sebastian D Eastham³, Evan M Gibney², William C Clark⁴, Noelle E Selin^{1,5}

¹ Institute for Data, Systems and Society, Massachusetts Institute of Technology, Cambridge, MA, United States of America

² Laboratory for Aviation and the Environment, Department of Aeronautics and Astronautics, Massachusetts Institute of Technology, Cambridge, MA, United States of America

³ Brahmal Vasudevan Institute for Sustainable Aviation, Department of Aeronautics, Imperial College London, London, United Kingdom

⁴ John F. Kennedy School of Government, Harvard University, Cambridge, MA, United States of America

⁵ Department of Earth, Atmospheric, and Planetary Sciences, Massachusetts Institute of Technology, Cambridge, MA, United States of America

E-mail: yuang007@mit.edu

This manuscript has been submitted for review in *Environmental Research Letters*. If accepted, the final version of this manuscript will be available via the ‘Peer-reviewed Publication DOI’ link on the right-hand side of the EarthArxiv web page for the paper.

Abstract. Organizational climate actions often prioritize greenhouse gas reductions without considering other impacts such as improved air quality from reduced fossil fuel use. While air quality benefits of large-scale policies are well studied, those of organization-level activities are more uncertain. We quantify the impact of organizations’ fossil fuel use from electricity purchasing and air travel on climate and air quality using a system-level approach, with data from two universities and one corporation based in greater Boston. We use energy system and aviation emission models to estimate marginal emissions of greenhouse gases and air pollution precursors, and compare monetized air quality impacts calculated using an atmospheric chemistry-transport model with climate impacts from the same activities. Organizational activities were associated with air quality damages of \sim \\$88/tCO₂ (electricity purchase) and \sim \\$265/tCO₂ (air travel), compared to \sim \\$170–200/tCO₂ in climate damages (2015 USD). Air quality impacts vary spatially, with renewable energy purchases and short-haul flight segments having proportionally more impacts in the US Northeast. Activities with the same CO₂ emissions can have very different overall monetized benefits, suggesting organizations seeking broader sustainability impacts should consider air quality alongside direct climate impacts.

Keywords: Organization, Air Quality, Decarbonization, Electricity purchase, Air travel

1. Introduction

Limiting the damages of anthropogenic climate change requires a rapid transition toward net-zero greenhouse gas emissions. Alongside national and international policies, commitments by organizations can help drive this transition [1–3]. Studies highlight CO₂ emission accounting and management as a first step towards broader corporate sustainability goals [4–6]. Polluting activities by organizations include direct emissions (scope 1), emissions from power usage (scope 2) and emissions along supply chains (scope 3) [7].

Carbon emission reductions can also impact other sustainability goals, such as improving air quality and health by reducing other fossil fuel related emissions. Exposure to atmospheric fine particulate matter (PM_{2.5}, particulate matter $\leq 2.5\mu\text{m}$ in diameter) leads to cardiovascular and respiratory diseases [8]. Exposure to ground-level ozone (O₃) also harms lung function, causes airway inflammation, and raises the risk of premature cardiopulmonary mortality [9]. Exposure to ambient PM_{2.5} and ozone contributed to an estimated 4.5 million deaths worldwide in 2019 [10]. Integrated modeling has been used to quantify the air pollution and health benefits of large-scale climate policies [11–17]. For example, Markandya et al. estimated using IAM and atmospheric chemistry-transport models that the health benefits of reduced air pollution from achieving the Paris Agreement targets (keeping global warming well below 2°C, ideally 1.5°C) could amount to \$54–\$110/tCO₂ [12]. Others have addressed impacts from specific CO₂-emitting sectors. For the energy sector, Dedoussi et al. found that the co-pollutant costs of carbon emissions from the US power sector are substantial, with associated air pollution health impacts resulting in \$44.7/tCO₂ in 2011 [18]. For aviation, Grobler et al. quantified its global marginal air quality impact to be \$114 (18-380)/tCO₂ [19].

Evaluations of organizational impacts have largely focused on CO₂, especially from actions addressing energy use and transportation (especially aviation) [2, 20–22]. For energy purchases, Egli et al. found that corporate initiatives like renewable energy procurement goals have a localized but growing impact, with potential to increase global renewable energy through expanded membership and stricter targets [2]. Arsenault et al. assessed the CO₂ and NO_x footprint of air travel at the Université de Montréal, calculating approximately 10.76 tonnes of CO₂ emissions per professor annually [20].

Like inter-governmental and national policies, organizational CO₂ reductions could also improve local and regional air quality by lowering ground-level PM_{2.5} and O₃. However, equivalent CO₂ reductions can yield different air quality outcomes, depending on when, where, and how emissions are reduced. Calculating air quality and health impacts from organizations requires spatial and temporal detail to account for pollutant chemistry, transport and regional conditions [11, 23]. Electricity use by organizations causes emissions and air pollution near energy generating units (EGUs) [24]. For air travel, emissions occur in origin, transit, and destination airports, as well as at altitude, with regional and global impacts on atmospheric chemistry that complicate emissions estimation [19].

Here, we focus on two prominent sectors often targeted by emission reduction efforts in organizations – electricity purchase (part of Scope 2 for greenhouse gas reduction initiatives) and air travel (scope 3) [2] – and compare their air quality and climate impacts. We use detailed energy consumption and flight data from two universities (Universities A and C) and one corporation (Corporate B) all headquartered in the greater Boston area to examine local and regional air quality impacts associated with CO₂ emissions from these sectors. We use a system-level modeling approach to capture spatial and temporal responses to the distribution of impacts. We quantify air quality impacts using a high-resolution atmospheric chemical transport model. We calculate and compare monetized climate and air quality impacts separately for each organization, and assess the sensitivity of these estimates to different assumptions and calculation methods. We conclude by examining the implications of incorporating air quality impacts into broader organizational sustainability strategies.

2. Method

We discuss data collection, modeling, and emission and impact attribution to organizations in the following sections. Supporting Information (SI) Figure S1 outlines our data and modeling framework. We first summarize data we collect from organizations (Section 2.1), including electricity consumption and air travel activity. To quantify emissions and their impacts on air quality and climate, we use several models. The electricity system is modeled using the US Electricity Generation Optimization (US-EGO) model (Section 2.2). Aviation emissions are estimated with the Aviation Emission Inventory Code (AEIC) described in Section 2.3. To evaluate air quality impacts, we use the GEOS-Chem High Performance (GCHP) model (Section 2.4), a three-dimensional chemical transport model that simulates spatially resolved PM_{2.5} and O₃ concentrations. For climate impacts, we calculate CO₂ emissions directly, and convert non-CO₂ impacts from aviation emissions into CO₂-equivalent terms using the Aviation Environmental Portfolio Management Tool–Impacts Climate (APMT-IC) introduced in Section 2.5. These outputs are used to estimate associated mortality and monetized air quality impact in Section 2.6, and monetized climate impact in Section 2.7. Finally, we describe our attribution of emissions, climate, and air quality impacts to specific organizations (Section 2.8).

2.1. Organizational Data

Table S1 summarizes the organizational characteristics of Universities A and C and Corporate B relevant to emissions and travel behavior. We obtain monthly electricity demand data from University A and Corporate B for 2022, including electricity usage by location and fuel mix. University A and C source electricity in the Northeast US, while Corporate B also has facilities in the Southeast US. For air travel, we obtain detailed records of employee flight legs from Corporate B’s internal records for 2021 and 2022,

and were provided by University C for 2019 based on data originally collected through an internal survey. We match flights to Official Aviation Guide (OAG) schedule data to identify aircraft type, route, and carrier [25]. Both data sets include only flights taken by employees in their official capacities (e.g., faculty, staff), and exclude student or visitor travel. Our primary focus for Corporate B is on its 2022 data, while we use data from 2021 as a complementary sensitivity test to account for potential COVID-related impacts.

2.2. Energy grid response model

The United States Electricity Generation Optimization (US-EGO) model, is an hourly power system optimization model that simulates least-cost electricity generation and inter-regional transmission across the contiguous US. This model outputs plant-level generation profile which allows us to estimate hourly emissions of CO₂, NO_x and SO₂ from individual EGUs. The model has been previously validated against the EPA’s Emissions and Generation Resource Integrated Database (eGRID) [26].

We update US-EGO based on the implementation by Jenn and Freese et al [26, 27], modifying it for compatibility with NumPy 4.11 and revising the renewable energy portfolio using data from EPA’s National Electric Energy Data System (NEEDS) version 5.16. Description of the model structure, data sources, and assumptions is provided in the SI.

2.3. Aviation Emissions

The Aviation Emission Inventory Code (AEIC) calculates aviation emissions for CO₂, NO_x, hydrocarbons (HC), and primary particulate matter (PM) using flight schedules, including emissions from landing and take-off (LTO) cycles, climbing, cruise and descending [28]. AEIC calculates flight distances using great-circle routes, adjusting for route inefficiency, and estimates fuel consumption and emissions per segment. AEIC inventories have been validated against other aviation emission inventories [28, 29] and are widely used in chemical transport models [30, 31].

2.4. Air quality modeling

We run full-chemistry simulations in GCHP v 14.1.1 [32–34], using a grid setup combining C48 (~200 km) global resolution and C180 (~50 km) regional resolution centered over the eastern US [35]. The C180 grid has a stretch factor of 3.6 and is centered at [37°N, 95°W] (Figure S3), enabling enhanced spatial resolution while maintaining computational efficiency. Meteorology is from MERRA-2 reanalysis from 2016 to 2022 [36]. We use 72 non-uniform vertical layers, from the surface to 0.01 Pa (~80 km altitude), and apply a six-month spin-up.

Emissions are processed using the Harmonized Emissions Component (HEMCO) [37]. Anthropogenic emissions in the continental US, except for SO₂ and NO_x from

EGUs, are based on a modified 2016 National Emissions Inventory (NEI), adjusted from NEI 2011 [38]. EGU emissions are replaced with those simulated by the US-EGO model in this study. For aviation, we apply AEIC 2019, a standard global emissions inventory [39]. For other global sources, we use the Community Emissions Data System (CEDs) version 2. All other emission sources follow GCHP 14.1.1 standard settings.

2.5. Reduced-form aviation climate model

We use APMT-IC to generate probabilistic estimates of monetized climate impacts from aviation. The model employs a quasi-Monte Carlo ensemble of 100,000 runs [19, 40, 41]. APMT-IC converts aviation CO₂ emissions to radiative forcing (RF) using an impulse response function. It then estimates the RF of non-CO₂ emissions using species-specific response functions [19, 40, 41]. These RF values are translated into temperature changes using a two-box land–ocean energy balance model. To account for future background warming, APMT-IC uses the Model for the Assessment of Greenhouse Gas Induced Climate Change version 6 (MAGICC6) to simulate temperature trajectories for each Representative Concentration Pathways (RCPs) [42]. Here, we use RCP4.5 due to its intermediate greenhouse gas trajectory and alignment with plausible policy and technological developments [43]. APMT-IC estimates monetized damages based on: 1) a modified version of the Howard and Sterner damage function [44], calibrated to match the valuation framework of Rennert et al. [45]; 2) and projections of future global income consistent with the OECD Shared Socio-Economic Pathways (SSP) [46].

2.6. Health outcome

We quantify air pollution related health impacts of organizational electricity purchase and air travel through changes in concentrations of ground-level PM_{2.5} and O₃. Mortality is calculated for each age group and grid cell using concentration-response functions (CRFs) that relate changes in pollutant concentration to relative mortality risk. For PM_{2.5}, we apply the Global Exposure Mortality Model (GEMM) CRF for non-communicable diseases and lower respiratory infections [47]. For O₃, we use a log-linear CRF for all-cause and respiratory mortality based on the maximum daily 8-hour average (MDA8-O₃) [48]. Further assumptions, equations, data sources, and uncertainty calculations are detailed in the SI.

2.7. Monetized impacts of emissions

We estimate monetized impacts of emissions due to the climate impacts they cause following Rennert et al. using \$185/tCO₂ in 2020 USD (\$171/tCO₂ in 2015 USD), based on a near-term risk-free 2% discount rate. We show the monetized climate impact based on the recommended 2% discount rate and test the sensitivity of climate impact with two different discount rates proposed in Rennert al. (\$74/tCO₂ for a 3% discount rate and \$284/tCO₂ for a 1.5% discount rate [45]). For health-related damages from air

pollution, we monetize premature mortality derived from Section 2.6 using the Value of a Statistical Life (VSL), scaled by country and year according to GDP per capita following Rennert et al. [45], with detailed calculations in the SI.

2.8. Emission and impact attribution

We use our model-based analysis to attribute emissions and resulting impacts to organizations based on their electricity purchases and air travel.

For electricity purchases, we simulate the baseline electricity system using US-EGO and re-run the simulation after subtracting each organization’s estimated hourly demand. The difference between the baseline and adjusted scenarios represents attributable emissions. This assumes that organizational purchases are marginal in the energy system, and we discuss implications of this assumption in Section 4. We also estimate the portion of fossil fuel energy use avoided through Corporate B’s renewable energy purchase, which supplies facilities in the greater Boston area.

For air travel, we attribute emissions and impacts per available seat kilometer (ASK), defined as the product of flight distance and the number of seats available on the aircraft. These are adjusted by typical load factors and distinguished between short- and long-haul segments. We assume that all passengers on a flight contribute equally, regardless of travel class or airline demand. This differs from other models that assign emissions by travel class (e.g., Travel Impact Model [49]). We also separately assess the impacts of short-haul flight legs (≤ 700 km) from University C departing Boston Logan International Airport, as these flights are potential candidates for emission reduction strategies through shifting to ground transport.

For both electricity and air travel, air quality attribution is conducted using GCHP simulations (Table S2) with and without the relevant emissions. To minimize numerical noise for small sources, we use emissions scaling factors in our GCHP simulations, consistent with previous studies [50]. Model assumptions, sensitivity analyses, and detailed attribution procedures are described in SI.

3. Results

We first examine the electricity grid generation and emissions induced by University A and Corporate B’s electricity purchase (Section 3.1.1). We then calculate the implications of these emissions for regional air quality (Section 3.1.2), and assess associated health outcomes and monetized climate and air quality impacts (Section 3.1.3). We examine characteristics of global air travel and air travel by Corporate B and University C in Section 3.2.1. We focus on CO₂, NO_x and other particulate emissions from air travel in Section 3.2.2, resulting air quality and mortalities in Section 3.2.3, and its monetized climate and air quality impacts in Section 3.2.4. We compare monetized impacts of electricity purchases and air travel in Section 3.3. Finally, we evaluate subsectors associated with potential emission reductions focusing on renewable

energy purchases and short-haul flight legs.

We report results at three spatial scales: (1) global, primarily for air travel, which has well-documented global air quality impacts due to cruise-altitude emissions and long-range transport [19, 51]; (2) the contiguous United States; and (3) the US Northeast (Connecticut, Maine, Massachusetts, New Hampshire, Rhode Island, and Vermont), where the studied organizations are headquartered. We present results normalized by tonnes of CO₂ emitted and electricity consumption for electricity purchase, and normalized by tonnes of CO₂ emitted and ASK for air travel. Per-tonne CO₂ normalization facilitates comparison with other carbon-emitting activities and climate damage estimates, while results per electricity consumption and ASK reflect the differences in operational efficiency and emissions intensity.

3.1. Electricity purchase impact

3.1.1. Electricity grid generation and emissions University A and Corporate B have comparable total electricity consumption in 2022 (150,000 MWh and 110,000 MWh respectively), but they receive electricity generated by different sources (Figure 1). University A sources over 80% of its electricity from natural gas plants in New England (Figure S4). Because of its facilities in the Southeast US, Corporate B’s energy mix comprises 61% coal and 35% natural gas, primarily from EGUs in North and South Carolina (Figures 1 and S4). Organizations’ electricity use is shaped by how the regional grid operates at the margin. University A’s reliance on natural gas in New England and Corporate B’s use of coal in the Carolinas align with our simulated grid response, which assumes that costlier fuels are dropped first to balance supply and demand (Figure S5) [52].

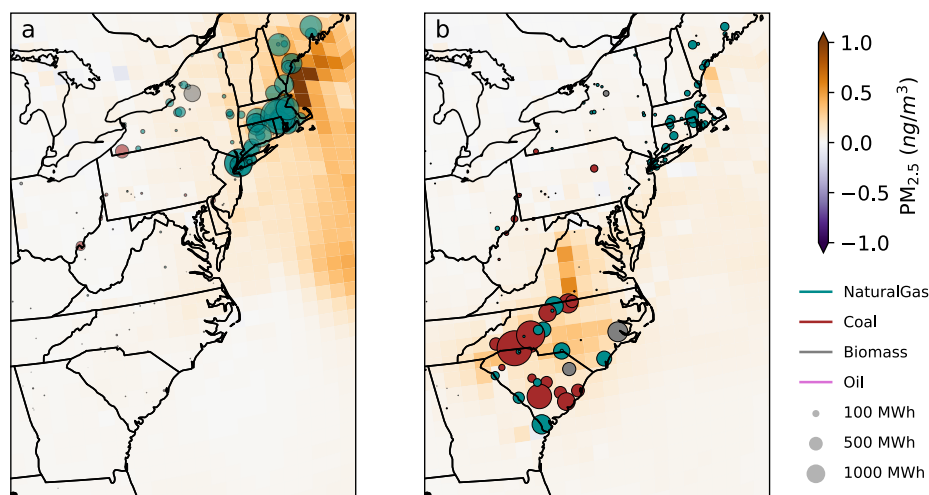


Figure 1. Electricity grid response to the electricity purchase by a) University A, and b) Corporate B and resulting annual-average induced ground-level PM_{2.5} concentration changes. Circles indicate an increase in electricity production from a single EGU.

The emissions intensity per kWh of electricity used by each organization differs from the US grid average (Table S3), reflecting variation in fuel mix and emission control technologies. The US electricity grid’s average CO₂ emission in US-EGO is 0.46 kg/kWh, consistent with previous findings by de Chalendar et al. (0.45 kg CO₂/kWh) [53]. CO₂ emissions are 0.50 and 0.67 kg/kWh for University A and Corporate B’s electricity purchase, respectively, higher than US grid average emissions due to greater reliance on natural gas and coal (Figure S4). NO_x and SO₂ emissions per kWh for University A and Corporate B are lower than the US grid average. Natural gas plants in New England and North Carolina have low NO_x emission rates (Figure S6), and coal-fired plants in North Carolina produce less SO₂ compared to other regions (Figure S7), due to advanced denitrification and desulfurization technologies [24].

We can further attribute EGU emissions from University A and Corporate B’s electricity purchases to a small number of fossil fuel EGUs in surrounding regions. Among EGUs supplying electricity to University A, the five with the highest NO_x emissions are associated with 15.9% of the electricity generation, 26.1% of CO₂ emissions (Figure S9), 50.9% of NO_x emissions (Figure S10) and 68.2% of SO₂ emissions (Figure S11) from University A’s electricity purchase. Four are natural gas plants commissioned in the 1970s with high NO_x and SO₂ emission factors, and their NO_x emissions have remained high until 2022. Similarly, among EGUs providing electricity to Corporate B, the five EGUs with the highest NO_x emissions are associated with 20.9% of electricity generation, 26.9% of CO₂ emissions, 34.5% of NO_x emissions and 30.8% of SO₂ emissions from Corporate B’s electricity purchase.

3.1.2. Air quality and mortality impact Figure 1 shows annual mean ground-level $PM_{2.5}$ concentrations attributable to organizational electricity purchases. We see localized elevated $PM_{2.5}$ concentrations of approximately $0.1 \text{ ng}/\text{m}^3$ around EGUs that generate electricity to meet organizations’ demand. For University A, emissions and resulting $PM_{2.5}$ are primarily in densely populated northeastern coastal regions, whereas $PM_{2.5}$ associated with Corporate B is over less populated areas [54]. As a result of these differences in the spatial extent of pollutant concentrations, the organizations’ impacts on population health differ, with premature mortalities in the US associated with University A’s electricity purchase 16% higher than that associated with Corporate B (Table S3).

Figure S13 shows the annual-mean ground-level $MDA8 - O_3$ concentrations attributable to organizational electricity purchases. Negative values near the Northeast coast for both organizations are largely influenced by the strong O₃ concentration decrease in winter. Seasonal analysis shows a decrease in winter O₃ levels (Figure S14) in the eastern US, which is under a NO_x-saturated regime, where an increase in NO_x leads to reduced O₃. Conversely, during the summer, the region transitions to a NO_x-limited regime, where increased NO_x emissions elevate O₃ concentrations (Figure S15). The ozone regime patterns are consistent with previous model simulations [26] and satellite observations [55]. There is a small fractional decrease in mortalities (Table S3)

associated with exposure to ground-level O₃ from *University A*'s electricity purchase, because of this O₃ reduction.

3.1.3. Monetized impact of electricity purchase by organizations Table S3 presents monetized climate and air quality impacts from the US electricity grid, and electricity purchase by different organizations. Values are in 2015 USD, with near-term 2% discount rate following [45]. Table S4 and Table S5 show climate impacts with 1.5% and 3% discount rates, and Table S6 and Table S7 show air quality impacts with 95% mortality uncertainty ranges.

Our baseline estimate of the monetized air quality impact from the US electricity grid is \$115.8 per tonne of CO₂ emitted, with PM_{2.5} and O₃ contributing \$96.0/tCO₂ and \$19.2/tCO₂, respectively. This is slightly higher than recent literature estimates: Thind et al. estimated a \$79/tCO₂ impact from the US electricity grid in 2014 [56], while Dedoussi et al. reported \$44.7/tCO₂ for the US electricity grid in 2011. Our higher estimate is largely driven by the use of an updated concentration-response function (CRF) from the Global Exposure Mortality Model (GEMM) [47] and an updated CRF for O₃ from Turner et al. which is approximately three times higher than those applied in earlier studies [48, 57].

Monetized air quality impacts from electricity purchase are \$75.3/tCO₂ for *University A* and \$101.5/tCO₂ for *Corporate B*, both of which are below the US electricity grid average. This is because regions surrounding *University A* and *Corporate B*, identified in Section 3.1.1, have cleaner power generation profiles than the US grid average (Figure S4). In the region where *University A* is located (NENGREEST: Massachusetts, Vermont, New Hampshire, Rhode Island), the grid average air quality impact is \$38/tCO₂, lower than that from *University A*'s electricity purchase. This is because the average NENGREEST region's electricity grid sources more electricity from nuclear, hydro and wind power (Figure S4(f)) compared to the energy source mix of *University A* (Figure S4(a)), where over 90% of electricity sources from natural gas. As shown in Figure S12, nuclear, hydro and wind power have lower NO_x and SO₂ emission rates compared to natural gas.

3.2. Air travel impact

3.2.1. Flight distance and transport capacity distributions Figure S17 (a, b) presents density plots for flight leg lengths and available seat kilometers (ASK) to compare global aviation patterns with air travel patterns of *Corporate B* and *University C*. Flight leg length distribution reflects the frequency of flight legs across different ranges, whereas the ASK distribution captures transport capacity, offering insights into emissions efficiency and resource allocation. Global air travel data show a strong concentration of flight legs in the range of 0–1500 km, while global ASK is more evenly spread across distances, emphasizing the importance of long-haul flight legs in overall capacity. While both *Corporate B* and *University C* exhibit similar patterns of flight legs in the range of

0-1500 km, their distributions diverge at longer distances. University C has a distinct secondary peak of flight legs in the 4,000–6,000 km range, likely driven by international academic collaborations, whereas Corporate B’s pattern aligns more closely with those of global aviation.

3.2.2. Air travel fuel burn and emissions To understand the spatial distribution of aviation-related climate and air quality impacts, we analyze fuel burn, which directly determines CO₂ and NO_x emissions. Figures S17 (c, d, e) show the spatial distribution of fuel burn for global aviation, Corporate B, and University C. The fuel burn distribution for all aviation is concentrated along major international corridors, particularly transatlantic routes and domestic routes in the USA, Europe, and China (Figure S17 (c)). Corporate B and University C show similar patterns, with high fuel burn densities around their headquarters and primary operational regions (Figure S17 (d,e)). However, University C exhibits a greater share of long-haul travel to Europe and Asia, reflecting its global academic collaborations, whereas Corporate B’s travel is more concentrated within North America. These differences in fuel burn distribution shape their respective emissions profiles.

Table S8 summarizes the fuel burn, CO₂, NO_x emissions, monetized climate and air quality impacts from global aviation, Corporate B and University C’s air travel. The emission values are normalized by ASK and emitted CO₂. We aggregate the global climate impact of NO_x, particulates, black carbon (BC), and hydrocarbons (HCs) and include them as non-CO₂ climate impacts in Table S8. We compare results for Corporate B in year 2021 and 2022 in Table S9.

We find that Corporate B’s air travel emitted 4000 tonnes of CO₂ (97.31 kg CO₂/kASK, where kASK refers to thousand ASK) in 2022. University C’s air travel emitted 710 tonnes of CO₂ (89.06 kg CO₂/kASK) in 2019. In comparison, we calculate that global commercial aviation emitted 826 million tons of CO₂ (79.51 kg CO₂/kASK) in 2019. University C’s travel results in a slightly lower CO₂/kASK than Corporate B, likely due to the greater proportion of long-haul flights in its mix. The altitude and latitude distribution of emissions (Figures S18 and S19) further highlight these differences. Corporate B’s emissions are more concentrated in mid-latitude regions and near the ground, while University C’s emissions are relatively larger at higher altitudes due to international travel.

3.2.3. Air quality and mortality impact Figure 2 presents ground-level annual mean PM_{2.5} concentrations attributable to global aviation, Corporate B, and University C’s air travel, normalized by their respective CO₂ emissions from air travel. Most atmospheric PM_{2.5} results from secondary aerosol formation via hemispheric-scale oxidation, so the spatial patterns mirror ambient precursor levels more than local flight activity [19]. As a result, regions with abundant aerosol precursors—such as East and Southeast Asia, Western Europe, and North America—exhibit the largest PM_{2.5} impacts, even in places with little flight activity. Organizational travel can also create localized hotspots.

Corporate B and University C’s flights cause elevated $\text{PM}_{2.5}$ in the greater Boston area (Figure 2 (g–i)), since about 50–70% of their flights depart or arrive there and additional fuel is burned during takeoff and landing. In contrast, aviation-induced O_3 perturbations are more diffuse globally (Figure S20), as tropospheric O_3 persists for hours to weeks—long enough to be transported far from emission regions before surface deposition.

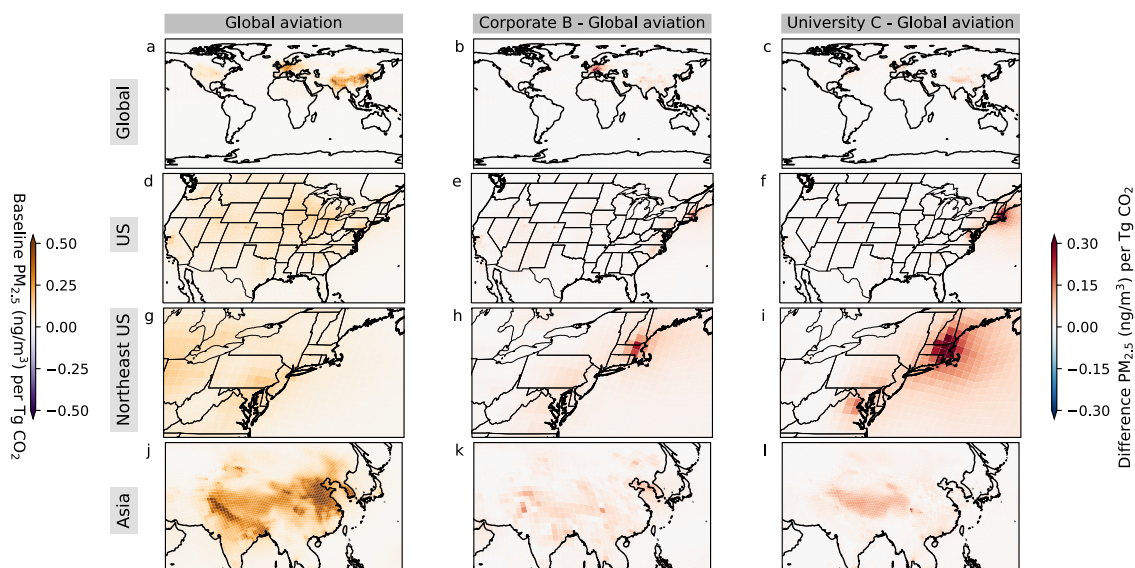


Figure 2. Ground-level changes in $\text{PM}_{2.5}$ concentration (ng/m^3) per teragram (Tg) of CO_2 emitted due to aviation activity. (a,d,g,j) show the changes in $\text{PM}_{2.5}$ attributed to global aviation (left axis). (b,e,h,k) show the difference in $\text{PM}_{2.5}$ between global aviation and Corporate B’s air travel (right axis). (c,f,i,l) show the difference in $\text{PM}_{2.5}$ between global aviation and University C air travel (right axis). Vertical stack shows different regions.

We estimate that degraded air quality from global air travel led to approximately 87,600 premature deaths globally in 2019 (Table S8). Notably, O_3 accounts for roughly 2–3 times more premature deaths than $\text{PM}_{2.5}$, reflecting updated concentration–response functions for ozone mortality [47, 48] and the high ozone formation efficiency of aircraft NO_x emissions at cruise altitudes [31, 58, 59]. Corporation B’s air travel in 2022 resulted in air quality impacts expected to cause an average of 0.38 deaths per year. For University C the comparable estimate is 0.074 deaths per year (Table S8).

The spatial distribution of mortality attributable to aviation emissions is governed by the combination of population density, background pollution, and local aviation fuel burn. Mortality impacts attributed to Corporate B’s and University C’s air travel show a similar spatial pattern to that of global aviation (Figures S21, S22, S23 panel (b)). Europe and North America have the highest mortality rate (mortalities attributable to aviation emissions divided by each country’s population) from aviation-related air pollution (Table S14).

3.2.4. Monetized impacts of air travel Table S8 summarizes monetized climate and air quality impacts of global aviation (2019) and of each organization’s air travel (values in 2015 USD, 2% discount rate). Climate impacts under 1.5% and 3% discount rates are in Tables S10 and S11, and uncertainty ranges for the air-pollution mortality impacts are in Tables S12 and S13.

We estimate the 2019 global aviation climate impact at \$168 billion (\$203.5/tCO₂), with 15% from non-CO₂ emissions. This is about three times the estimate by Grobler et al. [19], due to an updated climate damage function with a higher social cost of emissions [44], following Rennert et al. [45]; Dray et al. reported \$246/tCO₂ (2020 USD) using similar climate damage functions [60]. Corporate B’s 2022 air travel caused \$816,000 climate impact (\$19.9/kASK); University C’s 2019 travel caused \$143,000 (\$18.0/kASK). Both exceed the 2019 global average (\$16.2/kASK) by around 14%. Differences in climate impacts relative to the global average reflect variations in travel patterns, aircraft types, or routing efficiency.

For air quality, our analysis estimates a 2019 global aviation impact of \$211 billion (\$255.6/tCO₂). Air travel by organizations resulted in slightly higher air quality impact per ton of CO₂ (~\$265/tCO₂) for total damages of \$1.07 million for Corporate B in 2022 and \$186,000 for University C in 2019. Our results are more than twice as large as Grobler et al., who estimated a global marginal air quality impact of aviation emissions at \$114/tCO₂ [19], due to updated concentration-response functions for PM_{2.5} (Hoek et al. to Burnett et al.) and ozone (Jerrett et al. to Turner et al.) [47, 48].

The monetized health impact from aviation-related air pollution also varies across regions. The spatial pattern is determined by its mortalities combined with its VSL. Countries in Europe and North America experience the greatest per-capita impacts. In contrast, China’s per-capita monetized impact is about 70% of the global average, and India’s is only about 10%, reflecting lower VSL. Our calculations show similar patterns in mortality costs due to the emissions associated with air travel by both organizations (Figures S21, S22, S23 panel (a)).

3.3. Comparing monetized impacts of electricity purchase and air travel

We compare the relative air quality and climate impacts of emissions from electricity use and air travel by the organizations using their monetized values per tonne of CO₂ emitted (Figure 3), in 2015 USD. Each tonne of CO₂ incurs the same climate damages no matter where it is emitted; we adopt the figure of \$171 per tonne of CO₂ from Rennert et al. [45]. However, associated air quality impact varies. Air travel by organizations results in an air quality impact of ~\$265/tCO₂, nearly three times greater than the air quality impact from electricity purchase by organizations (\$75–100/tCO₂).

The spatial distribution of air quality impacts also differs between air travel and electricity purchases. Electricity emissions primarily affect regions near EGUs, where air pollution exposure is concentrated in areas with high population density and meteorological conditions that limit dispersion. In contrast, air travel emissions produce

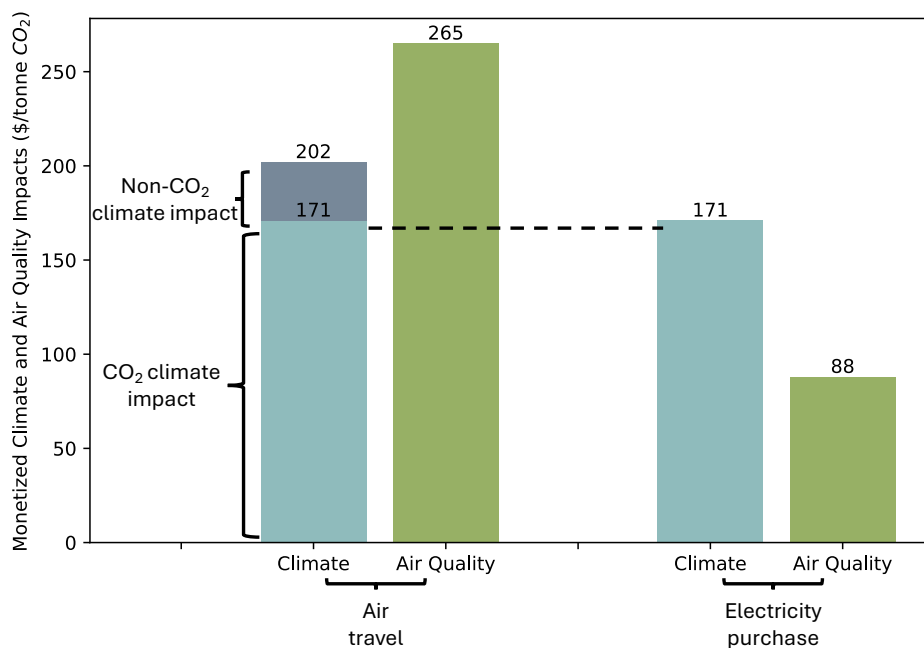


Figure 3. Average monetized climate and air quality impacts per tonne of carbon emitted of electricity purchase and air travel by organizations in this study. The range for air quality impact from electricity purchase is \$75-\$101/tCO₂; and the range for air quality impact from air travel is \$263-\$267/tCO₂. All values are in 2015 USD.

a more geographically disperse impact [19]. A large share (70%) of the total monetized damages from aviation impacts on air quality occurs outside the US – a share that is essentially the same for all aviation and for the flights taken by both organizations we studied.

3.4. Potential impact of emission reductions

We evaluate the impacts of subsets of organizational activities associated with two potential emission reduction strategies: (1) Corporate B’s potential renewable energy purchase, and (2) University C’s short-haul flight legs. Corporate B’s potential renewable energy purchase aims at displacing 10% of its electricity consumption (10,500 MWh). This fraction of energy use is associated with 5.22 Gg of CO₂ and associated co-pollutants (Table S3). The monetized climate benefit from this fraction of its emissions is \$893,000 (\$171/tCO₂). Air quality impacts of these emissions concentrate in the US Northeast, amounting to \$301,000 (\$57.63/tCO₂). Compared to Corporate B’s total electricity purchase, which yields \$101.49/tCO₂ of air quality benefits in the US and \$23.85/tCO₂ in the US Northeast, the electricity use targeted by its renewable energy purchase has an air quality impact per tonne of CO₂ that is 141% higher within the US Northeast.

University C’s short-haul flight legs represent a small subset of its overall travel (0.46 million ASK vs 7.94 million ASK total), but one which may be substitutable

by ground transport. Short-haul flight legs emit 0.06 Gg CO₂ (Table S8), but cause \$19,100 (\$316.45/tCO₂) in combined climate and air quality damages. Air quality damages contribute \$6,520 (\$108.24/tCO₂) globally, including \$47.35/tCO₂ in the US and \$33.32/tCO₂ in the US Northeast—68% higher than the air quality impact from University C’s total air travel in the US Northeast (\$19.8/tCO₂).

4. Discussion

Electricity purchases and air travel by organizations contribute to both climate change and air pollution. While the climate impact of a tonne of CO₂ contributes equally to climate change regardless of where or how it is emitted, associated air quality impacts vary widely by sector and location. Thus, for organizations seeking to reduce emissions, the same CO₂ reduction effort can yield different health outcomes depending on the activity and context. By integrating high-resolution modeling with detailed data on electricity and air travel, we assessed how organizational activities influence pollution exposure and public health. Differences in air quality damages between air travel and electricity purchase highlights the need to weigh local health outcomes alongside climate goals. As more organizations adopt net-zero targets [2], strategies that prioritize high-impact emission sources such as short-haul flights can deliver more near-term public health benefits. These findings support growing policy interest in targeted decarbonization, such as short-haul flight restrictions in France and the global expansion of green certificate programs [11, 61].

Our analysis assumes that electricity purchases influence emissions at the grid’s margin, where incremental changes typically impact high-emission, high-cost fossil fuel plants operating under a cost-minimizing dispatch framework. This marginal approach accurately captures short-term emissions responses to electricity purchase by organizations under the current grid structure, where fossil fuel plants remain the primary source of flexible generation [62, 63]. However, this approach may overestimate emissions for organizations without first-mover influence or operate in regions shifting toward renewables, as illustrated by the difference between University A’s electricity use (\$59/tCO₂) and the average grid where University A sits (\$38/tCO₂).

We assess air travel using direct flight emissions, excluding network effects. In practice, airline operations involve complex scheduling and hub structures [64], meaning that small reductions in demand may not immediately translate to fewer flights. Furthermore, this approach does not capture potential long-term adjustments by airlines, such as changes in schedules and routes due to sustained demand shifts. Nor does it address potential requirements for alternative modes of transportation if a mobility need cannot be suppressed. How demand shifts affect airline scheduling, fleets, or traveler modes remains uncertain and needs further analysis.

Future work could extend these estimates of organizations’ climate and air quality impacts to assess mitigation strategies, accounting for evolving electricity systems and airline operations. The impacts will also depend on shifts in energy and aviation

technologies (e.g., renewables, efficient engines), consumer behavior (e.g., building utilization, travel preferences), and population trends. Improved understanding of the role of organizational decisions shape emissions and pollution exposure can help inform more effective sustainability transitions.

Data availability statement

The data that support the findings of this study are openly available at the following URL/DOI: [10.5281/zenodo.15871924](https://doi.org/10.5281/zenodo.15871924).

Acknowledgments

This research is supported in part by Biogen, Inc., and Italy’s Ministry for Environment, Land and Sea through its gift to Harvard University’s Sustainability Science Program (WCC). The MERRA-2 data used in this research have been provided by the Global Modeling and Assimilation Office (GMAO) at NASA Goddard Space Flight Center. The computations presented here were conducted using the “Svante” cluster, a facility located at MIT’s Massachusetts Green High Performance Computing Center and supported by the MIT Center for Sustainability Science and Strategy (<https://cs3.mit.edu>).

References

- [1] A. Hsu, N. Höhne, T. Kuramochi, M. Roelfsema, A. Weinfurter, Y. Xie, K. Lütkehermöller, S. Chan, J. Corfee-Morlot, P. Drost, P. Faria, A. Gardiner, D. J. Gordon, T. Hale, N. E. Hultman, J. Moorhead, S. Reuvers, J. Setzer, N. Singh, C. Weber, and O. Widerberg. A research roadmap for quantifying non-state and subnational climate mitigation action. *Nat. Clim. Change*, 9(1):11–17, 2019.
- [2] F. Egli, R. Zhang, V. Hopo, T. Schmidt, and B. Steffen. The contribution of corporate initiatives to global renewable electricity deployment. *Nat. Commun.*, 14(1):4678, 2023.
- [3] R. G. Eccles, I. Ioannou, and G. Serafeim. The impact of corporate sustainability on organizational processes and performance. *Manag. Sci.*, 60(11):2835–2857, 2014.
- [4] E. G. Hertwich and R. Wood. The growing importance of scope 3 greenhouse gas emissions from industry. *Environ. Res. Lett.*, 13(10):104013, 2018.
- [5] M. Li, T. Wiedmann, and M. Hadjikakou. Enabling full supply chain corporate responsibility: Scope 3 emissions targets for ambitious climate change mitigation. *Environ. Sci. Technol.*, 54(1):400–411, 2020.
- [6] M. Brander, M. Gillenwater, and F. Ascui. Creative accounting: A critical perspective on the market-based method for reporting purchased electricity (scope 2) emissions. *Energy Policy*, 112:29–33, 2018.
- [7] Y. A. Huang, C. L. Weber, and H. S. Matthews. Categorization of scope 3 emissions for streamlined enterprise carbon footprinting. *Environ. Sci. Technol.*, 43(22):8509–8515, 2009.
- [8] Q. Di, Y. Wang, A. Zanobetti, Y. Wang, P. Koutrakis, C. Choirat, F. Dominici, and J. D. Schwartz. Air pollution and mortality in the medicare population. *N. Engl. J. Med.*, 376(26):2513–2522, 2017.
- [9] U.S. EPA. Integrated science assessment (isa) for ozone and related photochemical oxidants (final report, apr 2020), 2020. U.S. Environmental Protection Agency, Washington, DC, EPA/600/R-20/012.
- [10] GBD 2019 Risk Factors Collaborators. Global burden of 87 risk factors in 204 countries and territories, 1990–2019: a systematic analysis for the global burden of disease study 2019. *The Lancet*, 396(10258):1223–1249, 2020.
- [11] X. Huang, V. Srikrishnan, J. Lamontagne, K. Keller, and W. Peng. Effects of global climate mitigation on regional air quality and health. *Nat. Sustain.*, pages 1–13, 2023.
- [12] A. Markandya, J. Sampedro, S. J. Smith, R. Van Dingenen, C. Pizarro-Irizar, I. Arto, and M. González-Eguino. Health co-benefits from air pollution and mitigation costs of the paris agreement: A modelling study. *Lancet Planet. Health*, 2(3):e126–e133, 2018.

- [13] M. Li, D. Zhang, C. T. Li, K. M. Mulvaney, N. E. Selin, and V. J. Karplus. Air quality co-benefits of carbon pricing in china. *Nat. Clim. Change*, 8(5):398–403, 2018.
- [14] A. Bin Thaneya and A. Horvath. Exploring regional fine particulate matter (PM_{2.5}) exposure reduction pathways using an optimal power flow model: The case of the illinois power grid. *Environ. Sci. Technol.*, 57(21):7989–8001, 2023.
- [15] E. E. McDuffie, R. V. Martin, J. V. Spadaro, R. Burnett, S. J. Smith, P. O’Rourke, M. S. Hammer, A. van Donkelaar, L. Bindle, V. Shah, L. Jaeglé, G. Luo, F. Yu, J. A. Adeniran, J. Lin, and M. Brauer. Source sector and fuel contributions to ambient PM_{2.5} and attributable mortality across multiple spatial scales. *Nat. Commun.*, 12(1):3594, 2021.
- [16] J. Heo, P. J. Adams, and H. O. Gao. Public health costs of primary PM_{2.5} and inorganic PM_{2.5} precursor emissions in the united states. *Environ. Sci. Technol.*, 50(11):6061–6070, 2016.
- [17] H. Yang, A. T. Pham, J. R. Landry, S. A. Blumsack, and W. Peng. Emissions and health implications of pennsylvania’s entry into the regional greenhouse gas initiative. *Environ. Sci. Technol.*, 55(18):12153–12161, 2021.
- [18] I. C. Dedoussi, F. Allroggen, R. Flanagan, T. Hansen, B. Taylor, S. R. H. Barrett, and J. K. Boyce. The co-pollutant cost of carbon emissions: An analysis of the us electric power generation sector. *Environ. Res. Lett.*, 14(9):094003, 2019.
- [19] C. Grobler, P. J. Wolfe, K. Dasadhikari, I. C. Dedoussi, F. Allroggen, R. L. Speth, S. D. Eastham, A. Agarwal, M. D. Staples, J. Sabnis, et al. Marginal climate and air quality costs of aviation emissions. *Environ. Res. Lett.*, 14(11):114031, 2019.
- [20] J. Arsenault, J. Talbot, L. Boustani, R. Gonzalès, and K. Manaugh. The environmental footprint of academic and student mobility in a large research-oriented university. *Environ. Res. Lett.*, 14(9):095001, 2019.
- [21] Lynn Dray and Andreas Schafer. Making an impact: The influence of policies to reduce emissions from aviation on the business travel patterns of individual corporations. *Energy Policy*, 38(12):7634–7638, 2010.
- [22] Joachim Ciers, Aleksandra Mandic, Laszlo Daniel Toth, and Giel Op’t Veld. Carbon footprint of academic air travel: A case study in switzerland. *Sustainability*, 11(1):80, 2019.
- [23] A. L. Goodkind, C. W. Tessum, J. S. Coggins, J. D. Hill, and J. D. Marshall. Fine-scale damage estimates of particulate matter air pollution reveal opportunities for location-specific mitigation of emissions. *Proc. Natl. Acad. Sci. U.S.A.*, 116(18):8775–8780, 2019.
- [24] L. Henneman, C. Choirat, I. Dedoussi, F. Dominici, J. Roberts, and C. Zigler. Mortality risk from united states coal electricity generation. *Science*, 382(6673):941–946, 2023.

- [25] OAG Aviation Worldwide LLC. Oag yearly historic flight schedules, version v12, 2015.
- [26] L. M. Freese, G. P. Chossière, S. D. Eastham, A. Jenn, and N. E. Selin. Nuclear power generation phase-outs redistribute us air quality and climate-related mortality risk. *Nat. Energy*, 8(5):492–503, 2023.
- [27] A. Jenn. The future of electric vehicle emissions in the united states. Presented at the Transportation Research Board 97th Annual Meeting, Washington, DC, 2018. Paper No. 18-03325.
- [28] N. W. Simone, M. E. J. Stettler, and S. R. H. Barrett. Rapid estimation of global civil aviation emissions with uncertainty quantification. *Transp. Res. D Transp. Environ.*, 25:33–41, 2013.
- [29] S. C. Olsen, D. J. Wuebbles, and B. Owen. Comparison of global 3-d aviation emissions datasets. *Atmos. Chem. Phys.*, 13(1):429–441, 2013.
- [30] V. Shah, D. J. Jacob, R. Dang, L. N. Lamsal, S. A. Strode, S. D. Steenrod, K. F. Boersma, S. D. Eastham, T. M. Fritz, C. Thompson, et al. Nitrogen oxides in the free troposphere: Implications for tropospheric oxidants and the interpretation of satellite no₂ measurements. *Atmos. Chem. Phys.*, 23(2):1227–1257, 2023.
- [31] S. D. Eastham, G. P. Chossière, R. L. Speth, D. J. Jacob, and S. R. H. Barrett. Global impacts of aviation on air quality evaluated at high resolution. *Atmos. Chem. Phys.*, 24(4):2687–2703, 2024.
- [32] I. Bey, D. J. Jacob, R. M. Yantosca, J. A. Logan, B. D. Field, A. M. Fiore, Q. Li, H. Y. Liu, L. J. Mickley, and M. G. Schultz. Global modeling of tropospheric chemistry with assimilated meteorology: Model description and evaluation. *J. Geophys. Res. Atmos.*, 106(D19):23073–23095, 2001.
- [33] S. D. Eastham, M. S. Long, C. A. Keller, E. Lundgren, R. M. Yantosca, J. Zhuang, C. Li, C. J. Lee, M. Yannetti, B. M. Auer, T. L. Clune, J. Kouatchou, W. M. Putman, M. A. Thompson, A. L. Trayanov, A. M. Molod, R. V. Martin, and D. J. Jacob. GEOS-Chem High Performance (gchp v11-02c): A next-generation implementation of the GEOS-Chem chemical transport model for massively parallel applications. *Geosci. Model Dev.*, 11(7):2941–2953, 2018.
- [34] R. V. Martin, S. D. Eastham, L. Bindle, E. W. Lundgren, T. L. Clune, C. A. Keller, W. Downs, D. Zhang, R. A. Lucchesi, M. P. Sulprizio, R. M. Yantosca, Y. Li, L. Estrada, W. M. Putman, B. M. Auer, A. L. Trayanov, S. Pawson, and D. J. Jacob. Improved advection, resolution, performance, and community access in the new generation (version 13) of the high-performance GEOS-Chem global atmospheric chemistry model (gchp). *Geosci. Model Dev.*, 15(23):8731–8748, 2022.
- [35] L. Bindle, R. V. Martin, M. J. Cooper, E. W. Lundgren, S. D. Eastham, B. M. Auer, T. L. Clune, H. Weng, J. Lin, L. T. Murray, J. Meng, C. A. Keller, W. M. Putman, S. Pawson, and D. J. Jacob. Grid-stretching capability for the GEOS-Chem 13.0.0 atmospheric chemistry model. *Geosci. Model Dev.*, 14(10):5977–5997, 2021.

- [36] R. Gelaro, W. McCarty, M. J. Suárez, R. Todling, A. Molod, L. Takacs, C. A. Randles, A. Darmenov, M. G. Bosilovich, R. Reichle, et al. The modern-era retrospective analysis for research and applications, version 2 (merra-2). *J. Clim.*, 30(14):5419–5454, 2017.
- [37] C. A. Keller, M. S. Long, R. M. Yantosca, A. M. da Silva, S. Pawson, and D. J. Jacob. Hemco v1.0: A versatile, esmf-compliant component for calculating emissions in atmospheric models. *Geosci. Model Dev.*, 7(4):1409–1417, 2014.
- [38] B. Henderson and L. Freese. Preparation of geos-chem emissions from cmaq, 2021.
- [39] S. D. Eastham and T. Fritz. Technical guidance for the aeic 2019 aircraft emissions inventory. Technical report, Harvard University, March 2022. AEIC Technical Note v2022-03.
- [40] K. Marais, S. P. Lukachko, M. Jun, A. Mahashabde, and I. A. Waitz. Assessing the impact of aviation on climate. *Meteorol. Z.*, 17(2):157–172, 2008.
- [41] A. Mahashabde, P. Wolfe, A. Ashok, C. Dorbian, Q. He, A. Fan, S. Lukachko, A. Mozdzanowska, C. Wollersheim, S. R. H. Barrett, et al. Assessing the environmental impacts of aircraft noise and emissions. *Prog. Aerosp. Sci.*, 47(1):15–52, 2011.
- [42] M. Meinshausen, S. C. B. Raper, and T. M. L. Wigley. Emulating coupled atmosphere-ocean and carbon cycle models with a simpler model, MAGICC6—part 1: Model description and calibration. *Atmos. Chem. Phys.*, 11(4):1417–1456, 2011.
- [43] A. M. Thomson, K. V. Calvin, S. J. Smith, G. P. Kyle, A. Volke, P. Patel, S. Delgado-Arias, B. Bond-Lamberty, M. A. Wise, L. E. Clarke, et al. Rcp4.5: A pathway for stabilization of radiative forcing by 2100. *Clim. Change*, 109:77–94, 2011.
- [44] P. H. Howard and T. Sterner. Few and not so far between: A meta-analysis of climate damage estimates. *Environ. Resour. Econ.*, 68(1):197–225, 2017.
- [45] K. Rennert, F. Errickson, B. C. Prest, L. Rennels, R. G. Newell, W. Pizer, C. Kingdon, J. Wingenroth, R. Cooke, B. Parthum, D. Smith, K. Cromar, D. Diaz, F. C. Moore, U. K. Müller, R. J. Plevin, A. E. Raftery, H. Ševčíková, H. Sheets, J. H. Stock, T. Tan, M. Watson, T. E. Wong, and D. Anthoff. Comprehensive evidence implies a higher social cost of CO₂. *Nature*, 610(7933):687–692, 2022.
- [46] R. Dellink, J. Chateau, E. Lanzi, and B. Magné. Long-term economic growth projections in the shared socioeconomic pathways. *Glob. Environ. Change*, 42:200–214, 2017.
- [47] R. Burnett, H. Chen, M. Szyszkowicz, N. Fann, B. Hubbell, III Pope, C. A., J. S. Apte, M. Brauer, A. Cohen, S. Weichenthal, J. Coggins, Q. Di, B. Brunekreef, J. Frostad, S. S. Lim, H. Kan, K. D. Walker, G. D. Thurston, R. B. Hayes, C. C. Lim, M. C. Turner, M. Jerrett, D. Krewski, S. M. Gapstur, W. R. Diver, B. Ostro, D. Goldberg, D. L. Crouse, R. V. Martin, P. Peters, L. Pinault, M. Tjepkema, A. van Donkelaar, P. J. Villeneuve, A. B. Miller, P. Yin, M. Zhou, L. Wang, N. A. H.

- Janssen, M. Marra, R. W. Atkinson, H. Tsang, T. Q. Thach, J. B. Cannon, R. T. Allen, J. E. Hart, F. Laden, G. Cesaroni, F. Forastiere, G. Weinmayr, A. Jaensch, G. Nagel, H. Concin, and J. V. Spadaro. Global estimates of mortality associated with long-term exposure to outdoor fine particulate matter. *Proc. Natl. Acad. Sci. U.S.A.*, 115(38):9592–9597, 2018.
- [48] M. C. Turner, M. Jerrett, III Pope, C. A., D. Krewski, S. M. Gapstur, W. R. Diver, B. S. Beckerman, J. D. Marshall, J. Su, D. L. Crouse, et al. Long-term ozone exposure and mortality in a large prospective study. *Am. J. Respir. Crit. Care Med.*, 193(10):1134–1142, 2016.
- [49] Google. Travel impact model (tim), version 2.0.0. <https://github.com/google/travel-impact-model>, 2022. Released April 2022. Accessed September 28, 2024.
- [50] M. Qiu, Y. Weng, J. Cao, N. E. Selin, and V. J. Karplus. Improving evaluation of energy policies with multiple goals: Comparing ex ante and ex post approaches. *Environ. Sci. Technol.*, 54(24):15584–15593, 2020.
- [51] D. S. Lee, D. W. Fahey, A. Skowron, M. R. Allen, U. Burkhardt, Q. Chen, S. J. Doherty, S. Freeman, P. M. Forster, J. Fuglestedt, A. Gettelman, R. R. De León, L. L. Lim, M. T. Lund, R. J. Millar, B. Owen, J. E. Penner, G. Pitari, M. J. Prather, R. Sausen, and L. J. Wilcox. The contribution of global aviation to anthropogenic climate forcing for 2000 to 2018. *Atmos. Environ.*, 244:117834, 2021.
- [52] Q. Luo, F. Garcia-Menendez, H. Yang, R. Deshmukh, G. He, J. Lin, and J. X. Johnson. The health and climate benefits of economic dispatch in china’s power system. *Environ. Sci. Technol.*, 57(7):2898–2906, 2023.
- [53] J. A. de Chalendar, J. Taggart, and S. M. Benson. Tracking emissions in the us electricity system. *Proc. Natl. Acad. Sci. U.S.A.*, 116(51):25497–25502, 2019.
- [54] A. Jbaily, X. Zhou, J. Liu, T. H. Lee, L. Kamareddine, S. Verguet, and F. Dominici. Air pollution exposure disparities across us population and income groups. *Nature*, 601(7892):228–233, 2022.
- [55] J. Jung, Y. Choi, S. Mousavinezhad, D. Kang, J. Park, A. Pouyaei, M. Ghahremanloo, M. Momeni, and H. Kim. Changes in the ozone chemical regime over the contiguous united states inferred by the inversion of no_x and voc emissions using satellite observation. *Atmos. Res.*, 270:106076, 2022.
- [56] M. P. S. Thind, C. W. Tessum, I. L. Azevedo, and J. D. Marshall. Fine particulate air pollution from electricity generation in the us: Health impacts by race, income, and geography. *Environ. Sci. Technol.*, 53(23):14010–14019, 2019.
- [57] M. Jerrett, R. T. Burnett, III Pope, C. A., K. Ito, G. Thurston, D. Krewski, Y. Shi, E. Calle, and M. Thun. Long-term ozone exposure and mortality. *N. Engl. J. Med.*, 360(11):1085–1095, 2009.
- [58] S. D. Eastham and S. R. H. Barrett. Aviation-attributable ozone as a driver for

- changes in mortality related to air quality and skin cancer. *Atmos. Environ.*, 144:17–23, 2016.
- [59] H. Lee, S. C. Olsen, D. J. Wuebbles, and D. Youn. Impacts of aircraft emissions on the air quality near the ground. *Atmos. Chem. Phys.*, 13(11):5505–5522, 2013.
- [60] L. Dray, A. W. Schäfer, C. Grobler, C. Falter, F. Allroggen, M. E. J. Stettler, and S. R. H. Barrett. Cost and emissions pathways towards net-zero climate impacts in aviation. *Nat. Clim. Change*, 12(10):956–962, October 2022.
- [61] A. Txapartegi, I. Cazcarro, and I. Galarraga. Short-haul flights ban in france: Relevant potential but yet modest effects of ghg emissions reduction. *Ecol. Econ.*, 224:108289, 2024.
- [62] K. Siler-Evans, I. L. Azevedo, and M. G. Morgan. Marginal emissions factors for the us electricity system. *Environ. Sci. Technol.*, 46(9):4742–4748, 2012.
- [63] A. D. Hawkes. Estimating marginal CO_2 emissions rates for national electricity systems. *Energy Policy*, 38(10):5977–5987, 2010.
- [64] F. Allroggen, M. D. Wittman, and R. Malina. How air transport connects the world—a new metric of air connectivity and its evolution between 1990 and 2012. *Transp. Res. Part E: Logist. Transp. Rev.*, 80:184–201, 2015.

Supporting Information for

Air quality impacts of electricity purchase and air travel by organizations

Yuang Chen¹, Florian Allroggen², Sebastian D Eastham³, Evan M Gibney², William C Clark⁴, Noelle E Selin^{1,5}

¹Institute for Data, Systems and Society, Massachusetts Institute of Technology, Cambridge, MA, United States of America

²Laboratory for Aviation and the Environment, Department of Aeronautics and Astronautics, Massachusetts Institute of Technology, Cambridge, MA, United States of America

³Brahmal Vasudevan Institute for Sustainable Aviation, Department of Aeronautics, Imperial College London, London, United Kingdom

⁴John F. Kennedy School of Government, Harvard University, Cambridge, MA, United States of America

⁵Department of Earth, Atmospheric, and Planetary Sciences, Massachusetts Institute of Technology, Cambridge, MA, United States of America

This PDF file includes:

Supporting text

Tables S1 to S15

Figures S1 to S23

SI References

S1 Supporting Text

S1.1 US-EGO model description

The model has 64 regions, following the region specification in the Integrated Planning Model (IPM) [1]. We also acquire electricity demand for all 64 regions in the contiguous United States from Energy Information Administration (EIA), together with electricity transmission costs between each two regions. A baseline electricity generation map of the continental US across 64 IPM regions is shown in Figure S2. We apply the capacity, fuel type, generation costs, emission control technologies and other plant-specific characteristics for every EGU in the United States from the NEEDS v.5.16 for the year 2016. We collect plant-level NO_x and SO₂ emission data from Clean Air Markets Program Data, and plant commission time, fuel type, and location information from individual EGU’s webpages. Although our model year is 2016, many of the highest-emitting units—such as older natural gas plants—remain operational with limited retrofits, and thus continue to dominate emissions through 2022.

The optimization step is performed by the JuMP package written in the Julia programming language. The key optimization formula is as follows:

$$\min_{x^{gen}, x^{trans}} \left(\sum_{i=1}^N \sum_{t=1}^T x_{it}^{gen} c_{it}^{gen} + \sum_{i=1}^R \sum_{j=1, j \neq i}^R \sum_{t=1}^T x_{ijt}^{trans} c_{ijt}^{trans} \right) \quad (S1)$$

where x_{it}^{gen} and c_{it}^{gen} represent the generation amount and generation costs of EGU i at hour t , with T being the total number of hours (8760) in a typical year; x_{ijt}^{trans} and c_{ijt}^{trans} represent the transmission amount and relevant cost for electricity transmission between each two regions, with R meaning the total number of regions (64). The US-EGO optimization step has constraints as follow:

1. Generation constraints:

$$x_{it}^{gen} - x_i^{capacity} \times profile \leq 0 \quad \text{if } i \text{ is powered by solar} \quad (S2)$$

$$x_{it}^{gen} - x_i^{capacity} \times profile \times 0.85 \leq 0 \quad \text{if } i \text{ is powered by wind} \quad (S3)$$

$$x_{it}^{gen} - x_i^{capacity} \times 0.95 \leq 0 \quad \text{if } i \text{ is powered by nuclear} \quad (S4)$$

$$x_{it}^{gen} - x_i^{capacity} \leq 0 \quad \text{if } i \text{ is powered by other fuel} \quad (S5)$$

where $x_i^{capacity}$ is the maximum amount of electricity EGU i can generate; *profile* is the renewable profile (renewable energy resources of each hour in each region).

2. Transmission constraints:

$$x_{ijt}^{trans} - x_{ij}^{trans-limit} \leq 0$$

where $x_{ij}^{trans-limit}$ is the limit of electricity transmission from region i to region j , based on EIA data. Note that we isolate the Texas (ERCOT), Eastern and Western Interconnections by setting the transmission limit to 0.01 to represent the limitation in transmissions between these regions.

3. Equilibrium constraint:

$$\sum_{i=1}^{N_r} x_i^{gen} + \sum_{i=1, i \neq r}^R x_{ir}^{trans} - \sum_{j=1, j \neq r}^R x_{rj}^{trans} - L_r \geq 0, \quad \forall r \in R, t \in T$$

where N_r is the number of EGUs in region r , L_r is the electricity demand (load) in region r . This equilibrium is true for each region r at each time t .

S1.2 Health Outcome Details

We estimate premature mortality associated with changes in ground-level PM_{2.5} and O₃ concentrations by applying established concentration-response functions (CRFs) to gridded population and baseline mortality data. We use the Gridded Population of the World v4.11 dataset at 30 arc-second resolution [2]. Age-specific baseline mortality rates are obtained from the World Health Organization (WHO) [3]. Since the air quality modeling grid is coarser than the population grid, pollutant concentrations are spatially matched by assigning each population cell the pollutant level from the overlying coarser grid cell. Premature mortality for each grid cell and age group is calculated using the following equation:

$$\Delta M_i = M_0 \frac{RR_i - RR_0}{RR_0} \quad (S6)$$

where ΔM_i is the change in mortality under scenario i (with organization's impact), M_0 is the baseline number of mortalities (without organization's impact), RR_i is the relative risk from pollutant exposure in scenario i , and RR_0 is the baseline risk.

For PM_{2.5}, we apply the CRF from the Global Exposure Mortality Model (GEMM) for non-communicable diseases and lower respiratory infections [4]. For O₃, we estimate mortality due to both all-cause and respiratory diseases using the log-linear CRF based on annual mean MDA8-O₃ from Turner et al. [5], with relative risk estimates of 1.02 (95% CI: 1.01–1.04) and 1.12 (95% CI: 1.08–1.16), respectively.

We monetize premature mortality using a country- and year-specific Value of a Statistical Life (VSL), following the approach from Rennert et al. [6]:

$$VSL_{i,t} = VSL_{US,t}^{Base} \times \left(\frac{GDPpc_{i,t}}{GDPpc_{US,t}} \right)^{\epsilon_1} \quad (S7)$$

$$VSL_{US,t}^{Base} = VSL_{US,1990}^{Base} \times \left(\frac{y_{t,US}}{y_{1990,US}} \right)^{\epsilon_2} \quad (S8)$$

where i denotes country and t denotes year. $VSL_{US,1990}^{Base}$ is \$4.8 million (in 1990 USD), and $y_{1990,US}$ is the 1990 US per capita income (\$40,192). $GDPpc_{i,t}$ and $y_{t,US}$ are obtained from the World Bank and U.S. BEA, respectively. Elasticities are $\epsilon_1 = 1.0$ and $\epsilon_2 = 0.4$, as recommended in Rennert et al. Uncertainties in mortality estimates are derived from the reported confidence intervals of the CRFs. We propagate these ranges through all calculations to quantify the resulting uncertainty in monetized damages.

S1.3 Attribution methods and sensitivity analysis

This section provides detailed descriptions of the methods used to attribute emissions and impacts to organizational activities, covering electricity purchases, air travel, and their air quality impacts. It also presents sensitivity analyses conducted to test key assumptions in electricity purchase attribution.

S1.3.1 Attribution for electricity purchase

We first conduct a baseline electricity simulation, where we model electricity grid generation and emissions. Next, we convert monthly electricity demand from organizational data into hourly demand estimates by distributing monthly demand across all days, assuming that an organization’s fraction of regional demand remains constant for each hour. Regional electricity demand is generally about 10% lower on weekends compared to weekdays, and our method does not differentiate between weekends and weekdays, which may lead to an overestimate of weekend activities in a workplace setting. However, this difference has minimal effect on our emissions calculations, as weekend-weekday differences have only a minor effect on annual average pollution levels, which drive the monetized impacts we estimate. We re-run the US-EGO model after subtracting an organization’s hourly electricity demand from the total regional demand. The difference in generation and emissions between the baseline and adjusted simulations represent the portion attributable to the organization. Finally, we estimate the portion of fossil fuel energy use avoided by Corporate B’s renewable energy purchases (which covers facilities in the greater Boston area). We remove the portion of demand covered by Corporate B’s renewable energy purchase from baseline regional electricity demand in a separate US-EGO simulation and repeat the steps above.

S1.3.2 Sensitivity tests for electricity purchase

To evaluate the robustness of our findings on electricity grid generation, grid emissions, and their climate and air quality impacts, we design two sensitivity tests: *Steady* and *Ten*. These tests help assess the extent to which our conclusions hold under different assumptions about electricity consumption patterns. The *Steady* test examines the impact of an alternative hourly electricity purchasing distribution by assuming Corporate B’s total daily electricity consumption is evenly distributed across all hours. This represents an extreme scenario, providing insight into how variations in hourly demand might influence grid generation and emissions. By redistributing demand uniformly, we assess whether the temporal fluctuations in electricity consumption could alter the results. The *Ten* test addresses the potential non-linearity in grid responses

to electricity purchase by organizations by scaling Corporate B’s electricity demand up by a factor of ten. This stress test helps determine whether the relationships observed in the baseline situation remain valid when demand increases. In both cases, the US-EGO model simulates grid emissions based on the adjusted electricity demand, which then serves as input to the GCHP model to estimate changes in ground-level PM_{2.5} and O₃ concentrations.

Our results indicate that electricity grid responses to moderate changes in consumption are largely robust and exhibit linear behavior across different allocation strategies. Figure S16 presents the distribution of electricity generation and PM_{2.5} concentrations for the two sensitivity cases. The spatial patterns of grid emissions and air quality impacts in both *Steady* and *Ten* closely resemble those in the base case for Corporate B. The valuation of air quality impacts is \$101.48/tCO₂ for Corporate B in base case, \$96.59/tCO₂ in the *Steady* case, and \$75.61/tCO₂ in the *Ten* case. The lower valuation in the *Ten* case arises from the non-linear relationship between pollutant concentrations and health outcomes: as PM_{2.5} and O₃ levels increase, the marginal health burden per unit of pollution declines, leading to proportionally fewer attributable mortalities [4, 5].

S1.3.3 Attribution for air travel

For air travel, we first model the total impacts for each flight leg that is carrying employees of the organizations studied. We use the flight schedule data from organizations as input to AEIC to compute emissions, which are then processed in APMT-IC to estimate climate impacts and in GEOS-Chem for air quality impact. To attribute a share of these total impacts to each organization, we divide the cumulative impact of all relevant flight legs by the average number of seats available across those flight legs. We further adjust this estimate using a general load factor to account for partial occupancy, resulting in an estimate of per-passenger impact. Since we do not have access to load factor information for each flight separately, we adopt a uniform load factor of 80% for years in our analysis, indicating that, on average, 80% of seats are occupied, aligning with International Civil Aviation Organization (ICAO) 2017 reports [7]. Short-haul flight legs include a larger fraction of time in Landing and Taking-off (LTO) processes than long-haul flight legs, and those processes burn more fuel [8]. Using a uniform average load factor for all flight legs thus could lead to biased attribution. Therefore, we categorize flight legs into long-haul (greater than 700 km) and short-haul (less than 700 km) and separately compute impacts per passenger following steps stated above. These are aggregated and normalized by total kilometers flown to obtain impact per revenue passenger kilometer (RPK), then divided by the load factor to yield the organization’s air travel impact per available seat kilometer (ASK). Finally, we examine the share of emissions and health impacts attributable to University C’s short-haul flight legs (shorter than 700 km) out of Boston Logan International Airport, as those legs are candidates for potential emission reductions strategies through shifting to train travel.

S1.3.4 Air quality impact attribution

We conduct multiple GEOS-Chem simulations to isolate and assess the air quality impact of organizations' energy use and aviation activities. Air quality impact is measured as changes in ground-level concentrations of PM_{2.5} and O₃, and is highly dependent on background atmospheric chemistry conditions. We first simulate the baseline air quality using the *Base* simulation. Then, we subtract emissions due to the sector we are isolating and perform an additional simulation. The difference between these two simulations represents the air quality impact attributable to the selected activity. Table S2 summarizes the GEOS-Chem simulations performed in this analysis.

Because emissions from individual organizations are very small, simulations isolating their impacts can be affected by numerical noise, in particular in ISORROPIA II, a package used in GEOS-Chem for aerosol thermodynamical equilibrium [9], which has been observed previously [10]. To avoid this issue, we scale the EGU emissions from organizations by 100 and air travel emissions by 1000, adding these to baseline emissions before running GEOS-Chem. The resulting pollutant concentration differences are then scaled back by the same factors. This approach relies on the assumption of a linear relationship between small emission changes and pollutant concentrations, where non-linear effects are minimal. This assumption is commonly used in studies that apply adjoint methods that calculate air quality impacts [11, 12]. Despite this amplification, the scaled emissions differences remain less than 0.01% of total US EGU and global aviation emissions, ensuring that non-linear effects are negligible.

S2 Supporting Tables

Table S1: The characteristics of the organizations in this study

	University A	Corporate B	University C
Year	2022	2022	2019
Number of employees	5000-10000	5000-10000	500-1000
Electricity consumption (MWh)	1.47×10^5	1.11×10^5	-
Air travel flight legs	-	20439	2210
Air travel distance (million km)	-	32.86	6.37

Note 1: University C is not the whole university but rather a sizable unit within a university that does not run lots of lab machinery.

Note 2: The numbers of employees are from organizations' LinkedIn pages

Table S2: GEOS-Chem simulations

Simulation	Explanation	Emission Source	Emission Year	Purpose
Electricity Purchase				
Base	Baseline electricity grid emissions	US-EGO generated	2016	Main text analysis
University A	Baseline minus grid response to University A's electricity purchase	University A's electricity purchase	2016	Main text analysis
Corporate B	Baseline minus grid response to Corporate B's electricity purchase	Corporate B's electricity purchase	2022	Main text analysis
Green	Baseline minus grid response to renewable energy purchase by Corporate B	Corporate B's renewable electricity purchase	2022	Main text analysis
Steady	Baseline minus grid response to Corporate B's altered hourly purchase	Corporate B's electricity purchase	2022	Supplementary information
Ten	Baseline minus grid response to 10x Corporate B's electricity purchase	Corporate B's electricity purchase	2016	Supplementary information
Air Travel				
Base	Baseline aviation emissions	AEIC 2019 aviation emission inventory	2019	Main text analysis
Corporate B 2022	Baseline plus emissions by flights taken by Corporate B's employees (2022)	Corporate B's flights schedule data	2022	Main text analysis
Corporate B 2021	Baseline plus emissions by flights taken by Corporate B's employees (2021)	Corporate B's flights schedule data	2021	Supplementary information
University C	Baseline plus emissions by flights taken by University C's employees	University C's flights schedule data	2019	Main text analysis
NoShort	Baseline plus emissions by non short-haul flights taken by University C's employees that land in or take off from Boston	University C's flights schedule data	2019	Main text analysis

Table S3: Electricity consumption, associated emissions, and monetized climate and air quality impacts for the US electricity grid, University A, Corporate B, and Corporate B's renewable energy purchase. The column for Corporate B's renewable energy purchase reflects the avoided emissions and impacts from displacing fossil fuel-based electricity with renewable energy purchase by Corporate B.

	Unit	US Electricity Grid	University A	Corporate B	Corporate B's renewable energy purchase
Year		2016	2022	2022	2022
Electricity consumption	[MWh]	4.10×10^9	1.47×10^5	1.11×10^5	1.05×10^4
CO ₂ emitted	[Gg]	1.87×10^6	73.19	73.97	5.22
NO _x emitted	[Mg]	2.76×10^6	48.07	45.91	3.9
SO ₂ emitted	[Mg]	1.85×10^6	30.71	31.14	2.32
CO ₂ emitted	[kg/kWh]	0.46	0.5	0.67	0.49
NO _x emitted	[g/kWh]	0.67	0.33	0.41	0.37
SO ₂ emitted	[g/kWh]	0.45	0.21	0.28	0.22
	[\$]	3.19×10^{11}	1.25×10^7	1.26×10^7	8.93×10^5
Climate NPV	[\$/MWh]	77.95	85.12	114.18	84.62
	[\$/tCO ₂]	171	171	171	171
US PM _{2.5} mortalities	[count]	1.96×10^4	0.73	0.63	0.01
US O ₃ mortalities	[count]	4.05×10^3	-0.13	0.19	0.02
US Total mortalities	[count]	2.37×10^4	0.6	0.82	0.03
	[\$]	2.16×10^{11}	5.51×10^6	7.51×10^6	2.44×10^5
US AQ NPV	[\$/MWh]	52.78	37.5	67.77	23.13
	[\$/tCO ₂]	115.78	75.33	101.49	46.75
US NE PM _{2.5} mortalities	[count]	2.54×10^3	0.56	0.15	0.02
US NE O ₃ mortalities	[count]	409.54	-0.18	0.04	0.02
US NE Total mortalities	[count]	2.95×10^3	0.39	0.19	0.03
	[\$]	2.70×10^{10}	3.52×10^6	1.76×10^6	3.01×10^5
US NE AQ NPV	[\$/MWh]	6.59	23.94	15.92	28.52
	[\$/tCO ₂]	14.46	48.10	23.85	57.63
	[\$]	5.36×10^{11}	1.80×10^7	2.02×10^7	1.14×10^6
Total Climate+AQ NPV	[\$/MWh]	130.73	122.61	181.94	107.75
	[\$/tCO ₂]	286.78	246.33	272.49	217.75

Table S4: The climate impact from the US electricity grid and electricity purchase from organizations in this study with 3% discount rate

	Unit	US electricity grid	University A	Corporate B	Corporate B's renewable energy purchase
Year		2016	2022	2022	2022
	[\$]	1.38×10^{11}	5.42×10^6	5.47×10^6	3.86×10^5
Climate NPV	[\$/MWh]	33.73	36.83	49.41	36.62
	[\$/tCO ₂]	74	74	74	74

Table S5: The climate impact from the US electricity grid and electricity purchase from organizations in this study with 1.5% discount rate

	Unit	US electricity grid	University A	Corporate B	Corporate B's renewable energy purchase
Year		2016	2022	2022	2022
	[\$]	5.31×10^{11}	2.08×10^7	2.10×10^7	1.48×10^6
Climate NPV	[\$/MWh]	129.46	141.36	189.63	140.53
	[\$/tCO ₂]	284	284	284	284

Table S6: The air quality impact in the US from the US electricity grid and electricity purchase from organizations in this study with the lower 2.5% quantile mortality

	Unit	US electricity grid	University A	Corporate B	Corporate B's renewable energy purchase
Year		2016	2022	2022	2022
	[\$]	1.72×10^{11}	3.95×10^6	5.93×10^6	1.79×10^5
US AQ NPV	[\$/MWh]	41.98	26.85	53.56	16.99
	[\$/tCO ₂]	92.10	53.94	80.21	34.33

Table S7: The air quality impact in the US from the US electricity grid and electricity purchase from organizations in this study with the higher 2.5% quantile mortality

	Unit	US electricity grid	University A	Corporate B	Corporate B's renewable energy purchase
Year		2016	2022	2022	2022
	[\$]	2.61×10^{11}	7.13×10^6	9.10×10^6	3.09×10^5
US AQ NPV	[\$/MWh]	63.73	48.50	82.14	29.25
	[\$/tCO ₂]	139.80	97.44	123.01	59.10

Table S8: Flight activity, emissions, and associated climate and air quality impacts from all aviation world-wide and from air travel by organizations

	Unit	All aviation	Corporate B	University C	University C Short-haul
Year		2019	2022	2019	2019
Number of air travel legs	[count]	1.31×10^7	2.04×10^4	2.21×10^3	736
Available seat kilometer (ASK)	[thousand]	1.04×10^{10}	4.11×10^4	7.94×10^3	461.86
Flight leg distance	[million kilometers]	5.32×10^4	32.86	6.35	0.37
Average available seats per flight leg taken	[count]	195.37	161.66	247.13	100.16
Average revenue passenger seats per flight leg taken	[count]	156.30	129.33	197.70	80.13
Fuel burn	[Gg]	2.62×10^5	1.27	0.22	0.02
CO ₂ emission	[Gg]	8.26×10^5	4.00	0.71	0.06
NO _x emission	[Mg]	4.59×10^6	22.14	3.97	0.24
Fuel burn	[kg/kASK]	25.20	30.84	28.23	41.31
CO ₂ emission	[kg/kASK]	79.51	97.31	89.06	130.35
NO _x emission	[kg/kASK]	0.44	0.54	0.50	0.51
	[\$]	1.68×10^{11}	8.16×10^5	1.43×10^5	1.25×10^4
Climate NPV	[\$/kASK]	16.18	19.86	17.95	27.14
	[\$/tCO ₂]	203.49	204.09	201.53	208.22
	[\$]	1.43×10^{11}	6.92×10^5	1.21×10^5	1.03×10^4
CO ₂ NPV	[\$/kASK]	13.74	16.85	15.22	22.29
	[\$/tCO ₂]	172.74	173.14	170.87	170.98
	[\$]	2.54×10^{10}	1.24×10^5	2.17×10^4	2.24×10^3
Non-CO ₂ climate NPV	[\$/kASK]	2.44	3.01	2.73	4.85
	[\$/tCO ₂]	30.75	30.95	30.66	37.24
Global PM _{2.5} mortalities	[count]	2.25×10^4	0.11	1.95×10^{-2}	5.70×10^{-4}
Global O ₃ mortalities	[count]	6.51×10^4	0.27	5.45×10^{-2}	4.31×10^{-3}
Global Total mortalities	[count]	8.76×10^4	0.38	7.40×10^{-2}	4.88×10^{-3}
	[\$]	2.11×10^{11}	1.07×10^6	1.86×10^5	6.52×10^3
Global AQ NPV	[\$/kASK]	20.33	25.99	23.43	14.11
	[\$/tCO ₂]	255.63	267.04	263.08	108.24
US PM _{2.5} mortalities	[count]	1.52×10^3	9.05×10^{-3}	1.62×10^{-3}	1.99×10^{-4}
US O ₃ mortalities	[count]	5.23×10^3	2.56×10^{-2}	4.36×10^{-3}	1.12×10^{-4}
US Total mortalities	[count]	6.75×10^3	3.46×10^{-2}	5.98×10^{-3}	3.12×10^{-4}
	[\$]	6.18×10^{10}	3.17×10^5	5.47×10^4	2.85×10^3
US AQ NPV	[\$/kASK]	5.94	7.72	6.88	6.17
	[\$/tCO ₂]	74.75	79.29	77.29	47.35
US NE PM _{2.5} mortalities	[count]	253.57	2.02×10^{-3}	6.12×10^{-4}	1.62×10^{-4}
US NE O ₃ mortalities	[count]	839.91	4.71×10^{-3}	9.21×10^{-4}	5.76×10^{-5}
US NE Total mortalities	[count]	1.10×10^3	6.73×10^{-3}	1.53×10^{-3}	2.19×10^{-4}
	[\$]	1.00×10^{10}	6.16×10^4	1.40×10^4	2.01×10^3
US NE AQ NPV	[\$/kASK]	0.96	1.50	1.76	4.34
	[\$/tCO ₂]	12.10	15.40	19.82	33.32
	[\$]	3.79×10^{11}	1.88×10^6	3.29×10^5	1.91×10^4
Climate+AQ NPV	[\$/kASK]	36.51	45.84	41.38	41.25
	[\$/tCO ₂]	459.12	471.13	464.61	316.46

Note 1: The average revenue passenger per flight leg taken for Corporate B, University C, and University C Short-haul flight legs should be 1 after attribution – with only one employee on each flight leg. Instead we report the number of revenue seats for flights taken by employees to provide more information

Note 2: The values fluctuate around \$171/tCO₂ because the NPV of CO₂-related climate impact is estimated using APMT-IC with 10,000 Monte Carlo simulations, where small deviations may occur.

Table S9: Flight characteristics, emission, climate and air quality impact from air travel by Corporate B in year 2021 and 2022

	Unit	Corporate B	Corporate B
Year		2022	2021
Number of flight legs	[count]	2.04×10^4	1.06×10^4
Available seat kilometer (ASK)	[thousand]	4.11×10^4	1.64×10^4
Flight leg distance	[million kilometers]	32.86	13.09
Average available seats per flight leg taken	[count]	161.66	146.55
Average revenue seats per flight leg taken	[count]	129.33	117.24
Fuel burn	[Gg]	1.27	0.47
CO ₂ emission	[Gg]	4.00	1.48
NO _x emission	[Mg]	22.14	7.89
Fuel burn	[kg/kASK]	30.84	28.66
CO ₂ emission	[kg/kASK]	97.31	90.43
NO _x emission	[kg/kASK]	0.54	0.48
	[\$]	8.16×10^5	3.03×10^5
Climate NPV	[\$/kASK]	19.86	18.53
	[\$/tCO ₂]	204.09	204.88
	[\$]	6.92×10^5	2.56×10^5
CO ₂ NPV	[\$/kASK]	16.85	15.66
	[\$/tCO ₂]	173.14	173.13
	[\$]	1.24×10^5	4.70×10^4
Non-CO ₂ climate NPV	[\$/kASK]	3.01	2.87
	[\$/tCO ₂]	30.95	31.75
Global PM _{2.5} mortalities	[count]	0.11	0.05
Global O ₃ mortalities	[count]	0.27	0.10
Global Total mortalities	[count]	0.38	0.14
	[\$]	1.07×10^6	4.12×10^5
Global AQ NPV	[\$/kASK]	25.99	25.15
	[\$/tCO ₂]	267.04	278.15
US PM _{2.5} mortalities	[count]	9.05×10^{-3}	3.63×10^{-3}
US O ₃ mortalities	[count]	2.56×10^{-2}	1.03×10^{-2}
US Total mortalities	[count]	3.46×10^{-2}	1.40×10^{-3}
	[\$]	3.17×10^5	1.28×10^5
US AQ NPV	[\$/kASK]	7.72	7.81
	[\$/tCO ₂]	79.29	86.36
US NE PM _{2.5} mortalities	[count]	2.02×10^{-3}	7.22×10^{-4}
US NE O ₃ mortalities	[count]	4.71×10^{-3}	1.70×10^{-3}
US NE Total mortalities	[count]	6.73×10^{-3}	2.42×10^{-3}
	[\$]	6.16×10^4	2.21×10^4
US NE AQ NPV	[\$/kASK]	1.50	1.36
	[\$/tCO ₂]	15.40	14.99
	[\$]	1.88×10^6	7.18×10^5
Climate+AQ NPV	[\$/kASK]	45.84	43.68
	[\$/tCO ₂]	471.13	483.03

Table S10: The climate impact from global aviation and air travel from the organizations in this study with 3% discount rate

	Unit	All aviation	Corporate B	University C	University C Short-haul
Year		2019	2022	2019	2019
	[\$]	9.15×10^{10}	4.46×10^5	7.77×10^4	7.16×10^3
Climate NPV	[\$/kASK]	8.81	10.86	9.79	15.49
	[\$/tCO ₂]	110.80	110.89	109.92	118.86

Table S11: The climate impact from global aviation and air travel from the organizations in this study with 1.5% discount rate

	Unit	All aviation	Corporate B	University C	University C Short-haul
Year		2019	2022	2019	2019
	[\$]	2.71×10^{11}	1.32×10^6	2.30×10^5	1.97×10^4
Climate NPV	[\$/kASK]	26.11	32.15	28.90	42.68
	[\$/tCO ₂]	328.36	328.45	324.54	327.42

Table S12: The global, the US and the US Northeast (NE) air quality impact from global aviation and air travel from the organizations in this study with the lower 2.5% quantile mortality

	Unit	All aviation	Corporate B	University C	University C Short
Year		2019	2022	2019	2019
	[\$]	1.53×10^{11}	7.90×10^5	1.36×10^5	3.51×10^3
Global AQ NPV	[\$/kASK]	14.80	19.24	17.06	7.59
	[\$/tCO ₂]	186.11	196.50	191.62	58.25
	[\$]	4.47×10^{10}	2.31×10^5	3.99×10^4	2.21×10^3
US AQ NPV	[\$/kASK]	4.30	5.63	5.03	4.78
	[\$/tCO ₂]	54.07	57.50	56.44	36.65
	[\$]	7.24×10^9	4.45×10^4	1.04×10^4	1.58×10^3
US NE AQ NPV	[\$/kASK]	0.70	1.08	1.32	3.41
	[\$/tCO ₂]	8.77	11.08	14.77	26.19

Table S13: The global, the US and the US Northeast (NE) air quality impact from global aviation and air travel from the organizations in this study with the higher 2.5% quantile mortality

Scenario	Unit	All aviation	Corporate B	University C	University C Short
Year		2019	2022	2019	2019
	[\$]	2.68×10^{11}	1.35×10^6	2.36×10^5	9.08×10^3
Global AQ NPV	[\$/kASK]	25.82	32.96	29.71	19.65
	[\$/tCO ₂]	324.78	336.63	333.55	150.77
	[\$]	7.88×10^{10}	4.02×10^5	6.93×10^4	3.50×10^3
US AQ NPV	[\$/kASK]	7.58	9.79	8.73	7.57
	[\$/tCO ₂]	95.36	100.05	98.01	58.08
	[\$]	1.27×10^{10}	7.71×10^4	1.76×10^4	2.44×10^3
US NE AQ NPV	[\$/kASK]	1.23	1.88	2.21	5.28
	[\$/tCO ₂]	15.43	19.17	24.84	40.50

Table S14: Mortalities associated with impacts of flight on air quality for 15 countries with the highest health costs

Country	Mortalities	Per capita mortalities	Percentage of global mortalities	Per capita mortalities compared to global average
Unit	count	10^{-5} count	%	
USA	6766.56 (4886.52 - 8640.90)	21.05 (15.20 - 26.88)	7.73	1.77
China	20873.51 (15491.79 - 26254.21)	15.17 (11.26-19.08)	23.84	1.28
Japan	4357.48 (3096.39 - 5611.81)	34.43 (24.46 - 44.34)	4.98	2.90
Germany	2427.99 (1848.89 - 3008.90)	30.84 (23.48 - 38.22)	2.77	2.60
UK	1867.08 (1377.74 - 2355.73)	28.85 (21.29 - 36.40)	2.13	2.43
France	1287.18 (960.38 - 1614.13)	19.99 (14.91 - 25.07)	1.47	1.68
Italy	1377.26 (1021.29 - 1733.07)	22.82 (16.93 - 28.72)	1.57	1.92
India	20688.42 (14846.95 - 26498.41)	15.78 (11.32 - 20.21)	23.63	1.33
Spain	1194.84 (854.99 - 1533.37)	25.98 (18.59 - 33.34)	1.36	2.19
South Korea	804.12 (600.70 - 1007.46)	16.27 (12.16 - 20.39)	0.92	1.37
Canada	518.24 (370.40 - 665.47)	15.19 (10.86 - 19.51)	0.59	1.28
Netherlands	424.15 (321.63 - 526.95)	25.59 (19.40 - 31.79)	0.48	2.16
Switzerland	183.19 (138.71 - 227.79)	23.53 (17.82 - 29.26)	0.21	1.98
Belgium	352.96 (264.85 - 441.16)	32.56 (24.43 - 40.70)	0.40	2.74
Russia	1131.29 (825.00 - 1436.58)	7.89 (5.75 - 10.01)	1.29	0.66
Rest of the world	23303.65 (16772.80 - 29802.65)	6.35 (4.57 - 8.12)	26.62	0.54
Global	87557.92 (63679.03 - 111358.58)	11.86 (8.63 - 15.09)	100	1

Table S15: Health costs associated with impacts of flight on air quality for 15 countries with the highest health costs

Country	Health costs	Per capita health costs	Percentage of global health costs	Per capita health costs compared to global average
Unit	10 ⁹ USD	USD	%	
USA	61.87 (44.68 - 79.01)	192.50 (139.01 - 245.82)	29.29	6.73
China	26.96 (20.01 - 33.90)	19.59 (14.54 - 24.64)	12.76	0.68
Japan	24.54 (17.44 - 31.60)	193.88 (137.77 - 249.70)	11.62	6.77
Germany	16.08 (12.24-19.92)	204.20 (155.50 - 254.06)	7.61	7.13
UK	13.52 (9.98-17.06)	208.97 (154.20 - 263.67)	6.40	7.30
France	7.60 (5.67 - 9.53)	118.02 (88.06 - 148.00)	3.60	4.12
Italy	6.71 (4.98 - 8.44)	111.20 (82.46 - 139.92)	3.18	3.89
India	5.30 (3.80 - 6.79)	4.04 (2.90 - 5.18)	2.51	0.14
Spain	4.96 (3.55 - 6.36)	107.79 (77.13 - 138.33)	2.35	3.77
South Korea	3.72 (2.78 - 4.66)	75.34 (56.28 94.39)	1.76	2.63
Canada	3.64 (2.60 - 4.67)	106.70 (76.27 - 137.02)	1.72	3.73
Netherlands	3.09 (2.34 - 3.84)	186.30 (141.27 231.45)	1.46	6.51
Switzerland	2.47 (1.87 - 3.08)	317.65 (240.53 - 394.98)	1.17	11.10
Belgium	2.33 (1.75 - 2.91)	215.10 (161.41 - 268.85)	1.10	7.52
Russia	1.70 (1.24 - 2.16)	11.83 (8.63 - 15.02)	0.80	0.41
Rest of the world	26.72 (19.34 - 34.08)	7.28 (5.27 - 9.29)	12.65	0.25
Global	211.21 (154.26 - 268.03)	28.62 (20.90 - 36.32)	100	1

S3 Supporting Figures

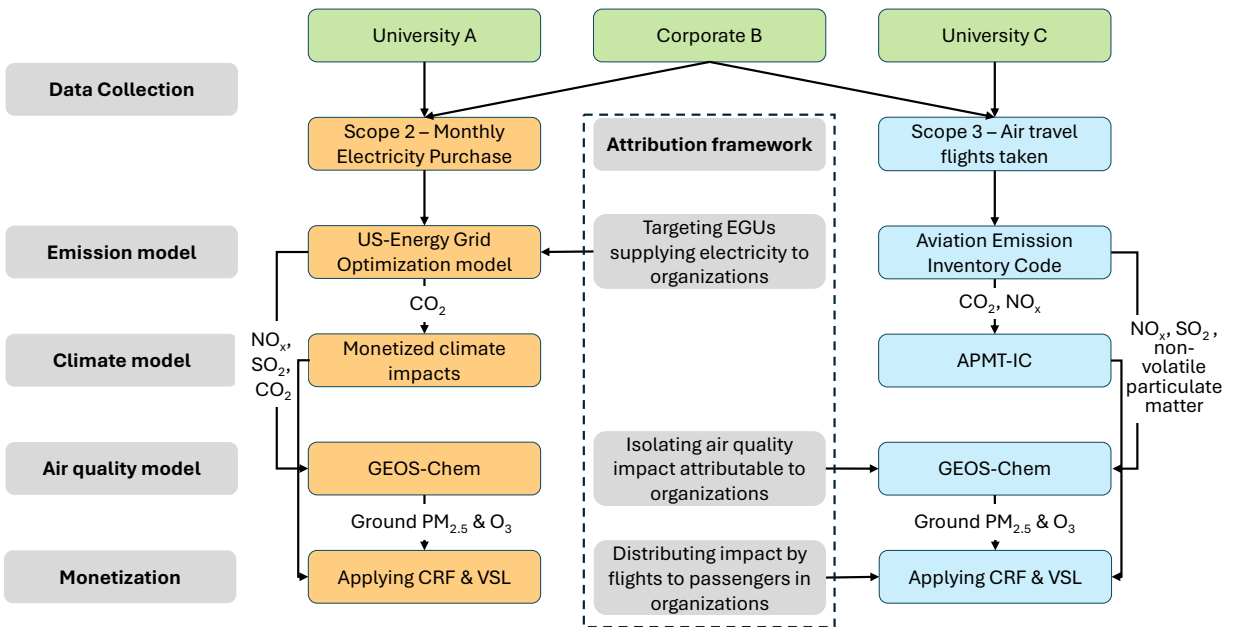


Figure S1: Methodological framework for quantifying the climate and air quality impact of scope 2 electricity purchase and scope 3 air travel by organizations including data collection, modeling, and attribution. EGU: Energy Generating Unit; APMT-IC: Aviation Environmental Portfolio Management Tool-Impacts Climate; CRF: Concentration Response Function; VSL: Value of a Statistical Life.

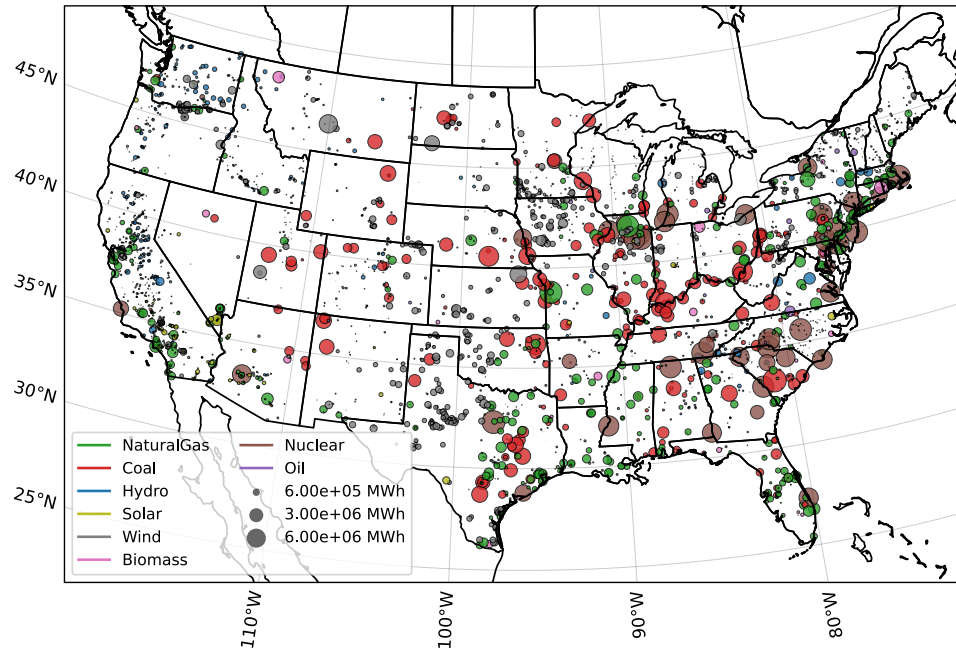


Figure S2: Baseline total generation of each generating unit of each fuel type in 2016.

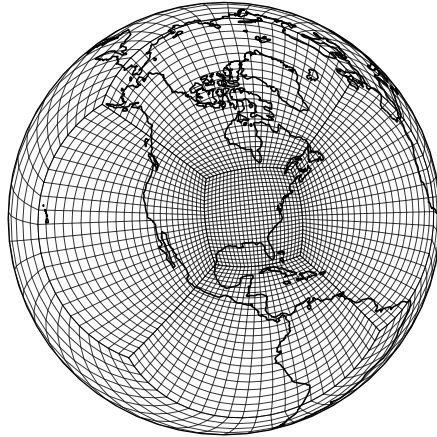


Figure S3: Stretched-grid structure in GEOS-Chem High Performance configured in this study, with center longitude 95°W , center latitude 37°N , stretch factor set as 3.6.

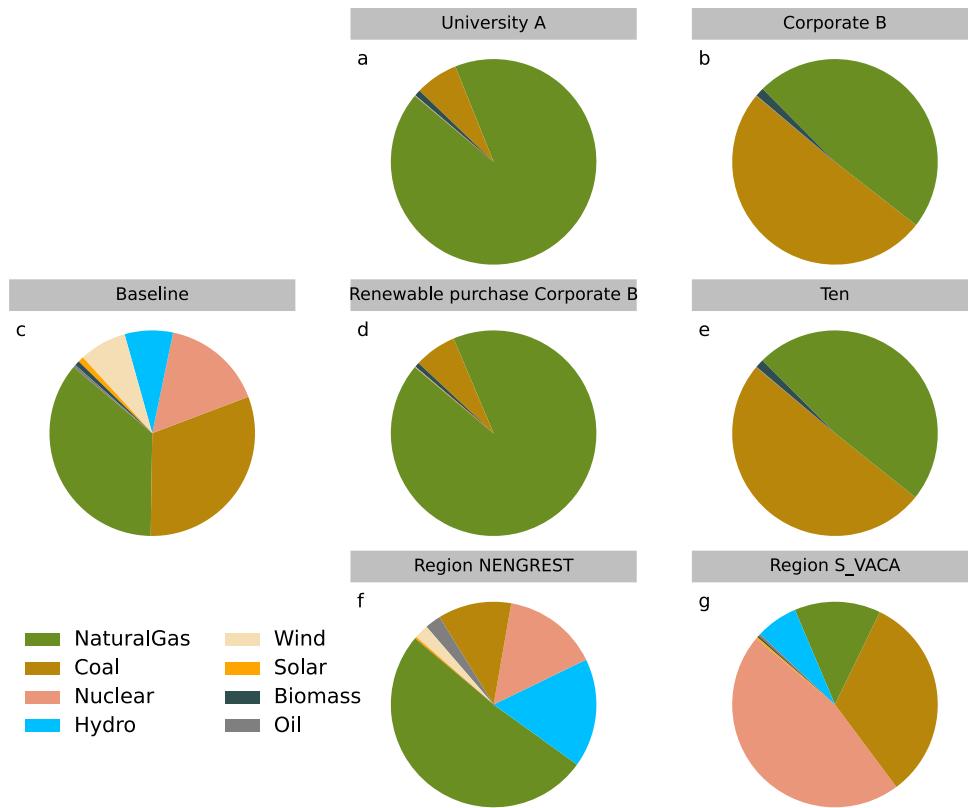


Figure S4: The fuel composition in baseline and regional electricity grid and each organization's electricity purchase: a) University A; b) Corporate B; c) Baseline electricity grid; d) Renewable purchase by Corporate B; e) Ten times of Corporate B's electricity purchase; f) the NENGREST region; g) the S_VACA region; where NENGREST and S_VACA are regions in IPM and are regional public grid where University A and Corporate B purchases electricity from

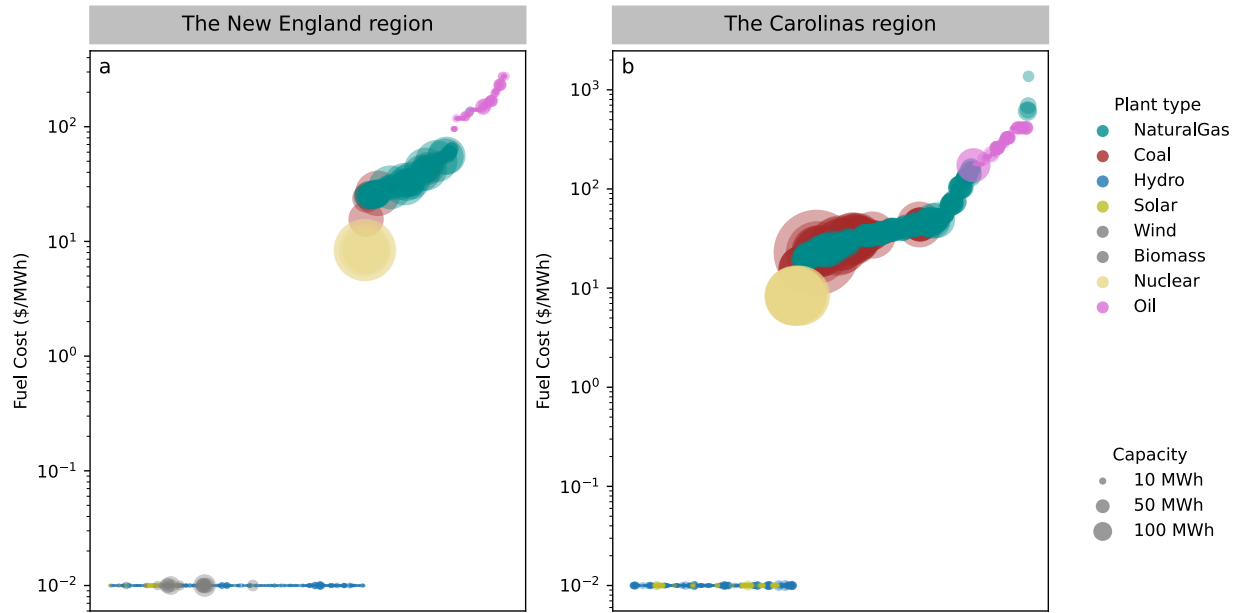


Figure S5: Fuel prices of individual power plants in regions where the analyzed organizations are located. Panel (a) displays fuel prices for the New England region (Connecticut, Maine, Massachusetts, New Hampshire, Rhode Island, and Vermont), and panel (b) for the Carolinas region (North and South Carolina). Plants are ranked on the x-axis by fuel cost. For modeling purposes, hydro, solar, and biomass plants—despite having zero fuel costs—are assigned a nominal value of \$0.01/MWh to ensure numerical stability.

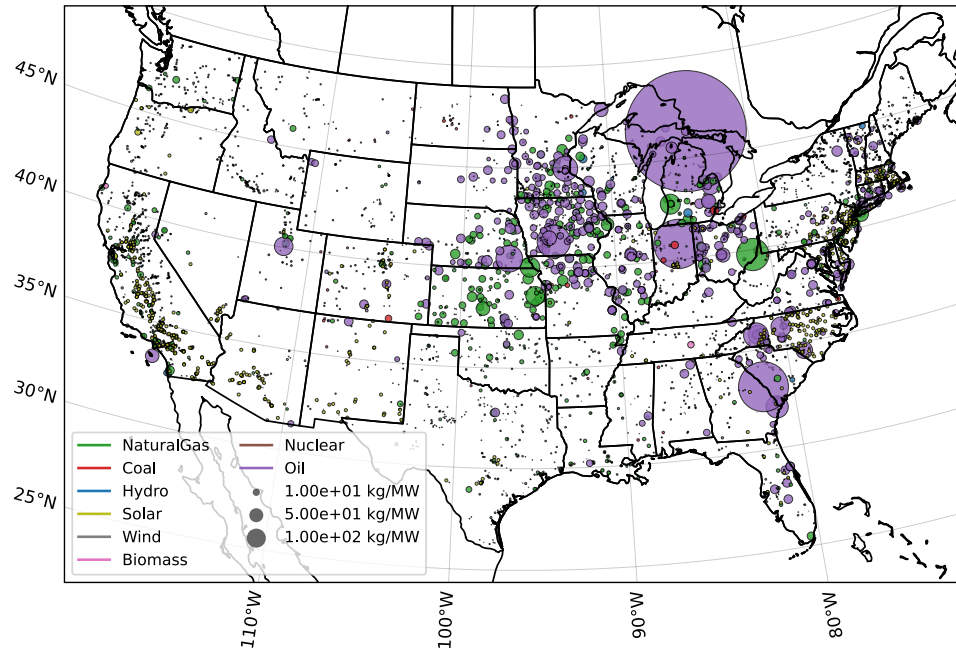


Figure S6: The NO_x emission factor for each energy generating unit in the US electricity grid

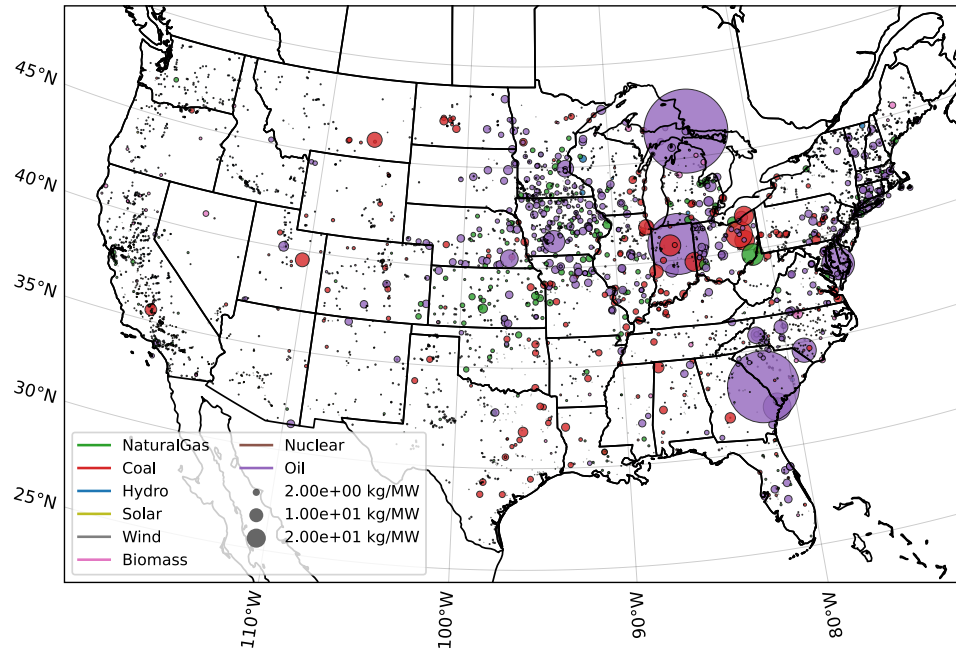


Figure S7: The SO₂ emission factor for each energy generating unit in the US electricity grid

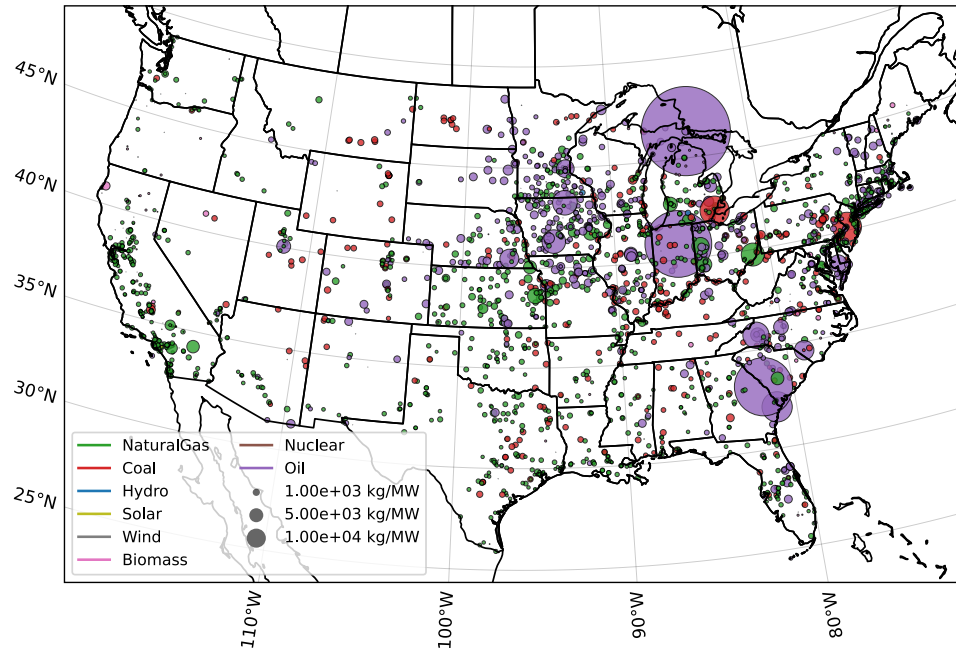


Figure S8: The CO₂ emission factor for each energy generating unit in the US electricity grid

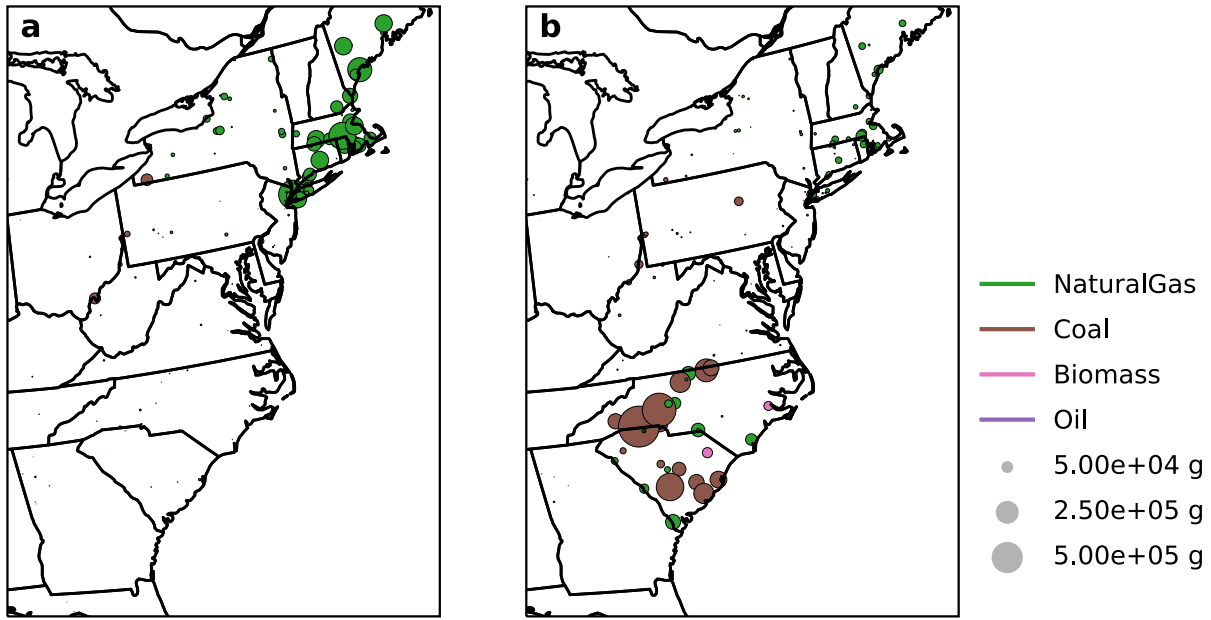


Figure S9: Total CO₂ emissions from electricity purchase from a) University A and b) Corporate B in 2022

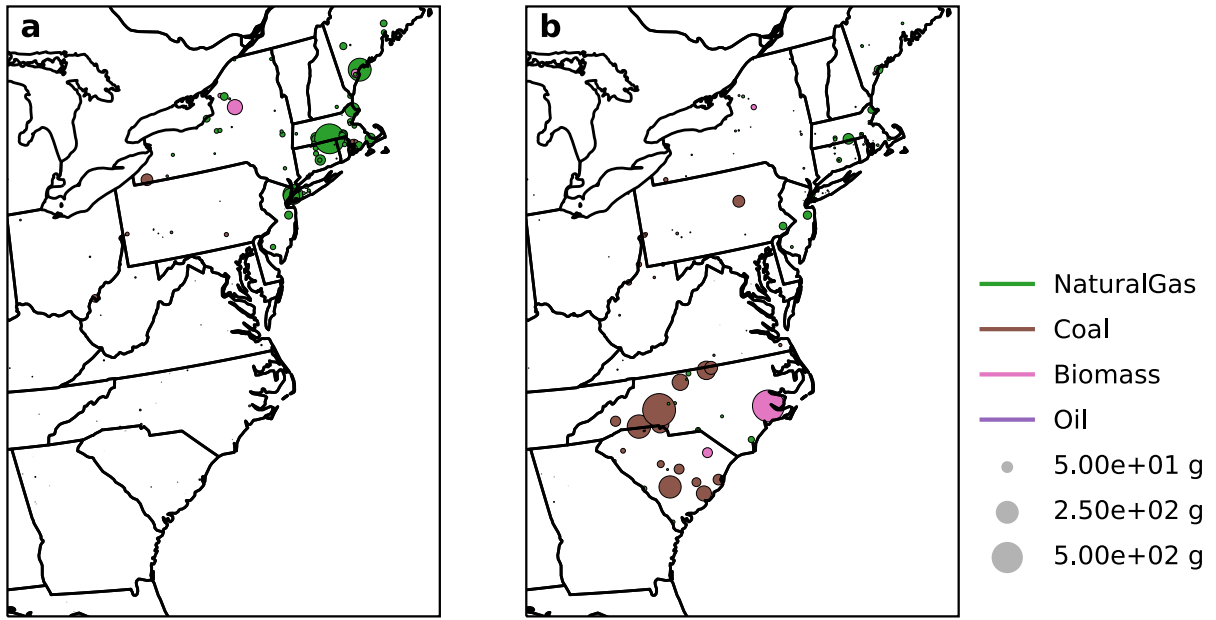


Figure S10: Total NO_x emissions from electricity purchase from a) University A and b) Corporate B in 2022

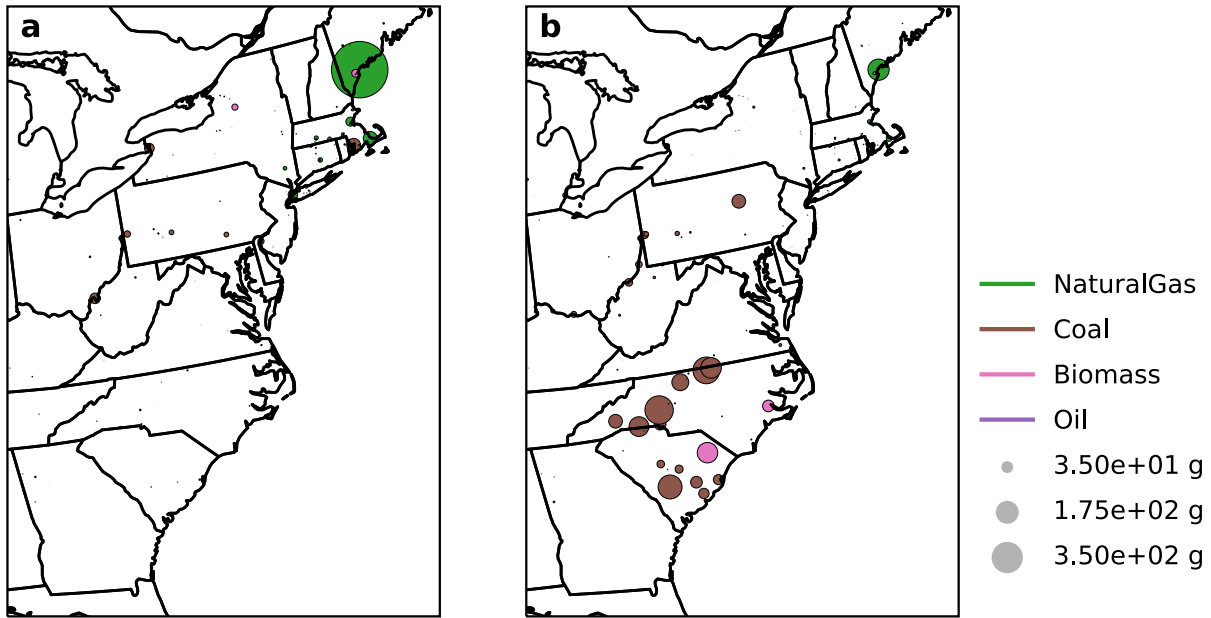


Figure S11: Total SO₂ emissions from electricity purchase from a) University A and b) Corporate B in 2022

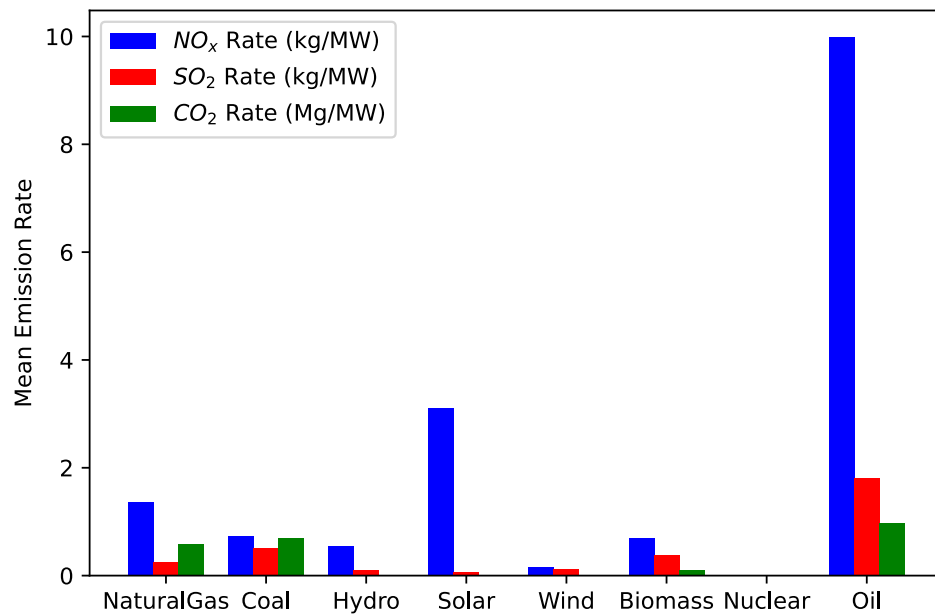


Figure S12: Average emission factors for CO₂, NO_x and SO₂ of each fuel type in the US electricity grid

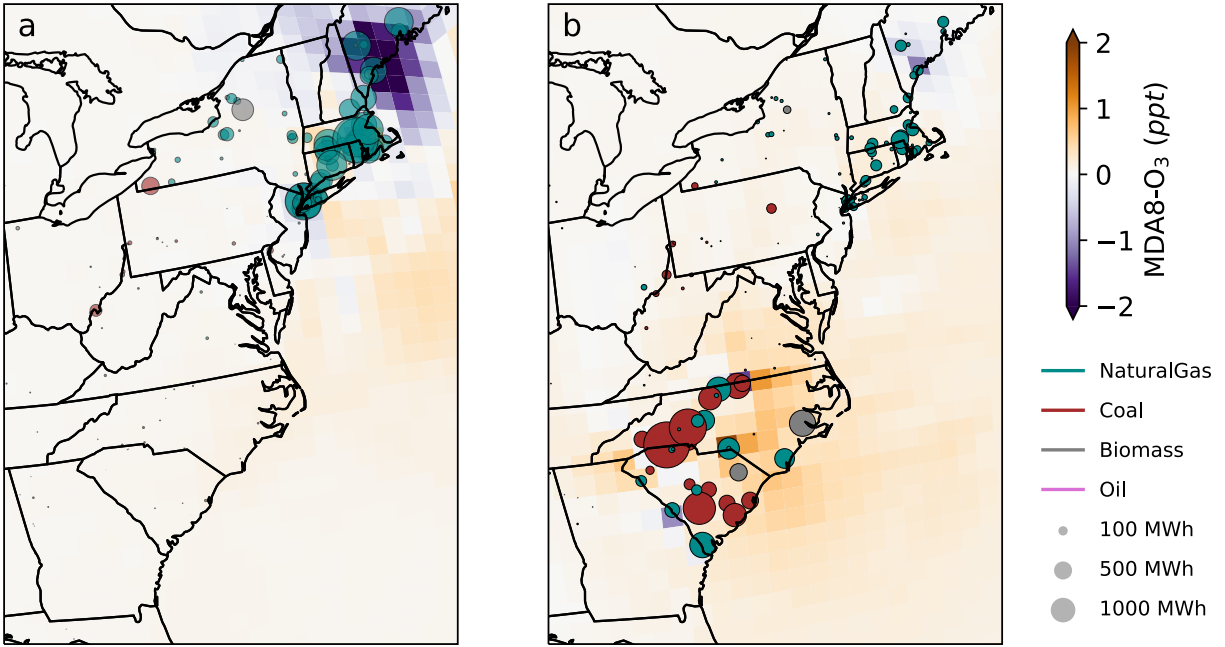


Figure S13: The electricity grid response and the yearly-average induced ground-level MDA8-O₃ (maximum daily 8-hour average) concentration from electricity purchase by a) University A, and b) Corporate B

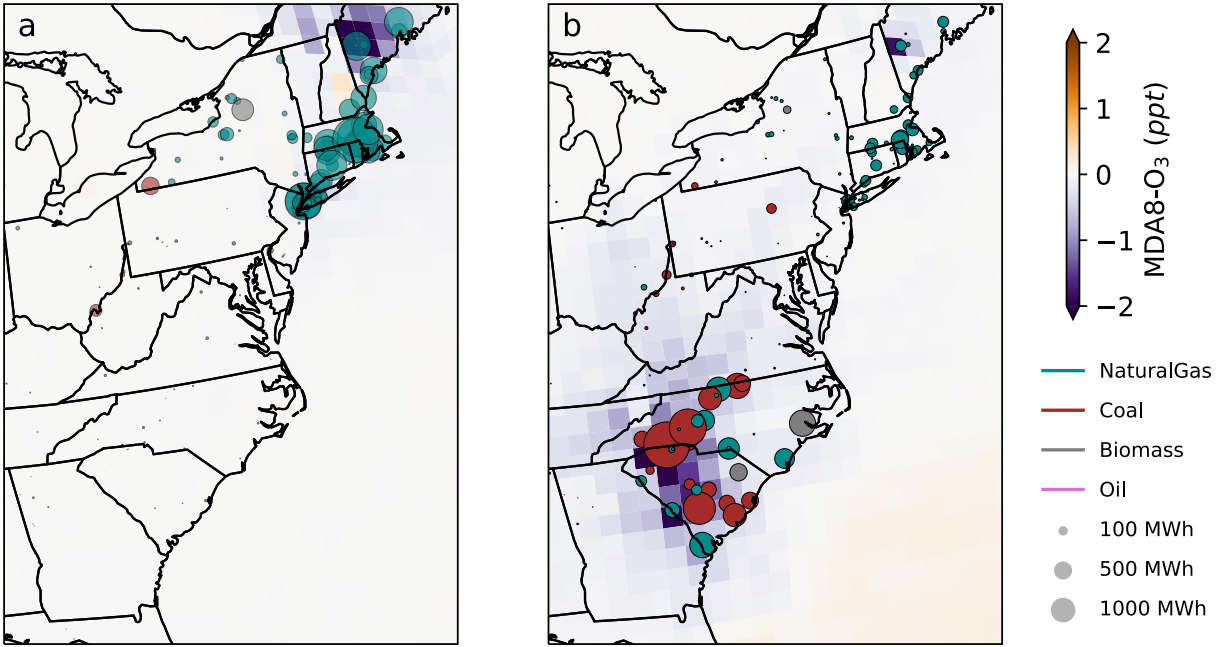


Figure S14: The electricity grid response and the induced seasonal average ground-level MDA8-O₃ (maximum daily 8-hour average) concentration for December, January and February (DJF) from electricity purchase by a) University A, and b) Corporate B

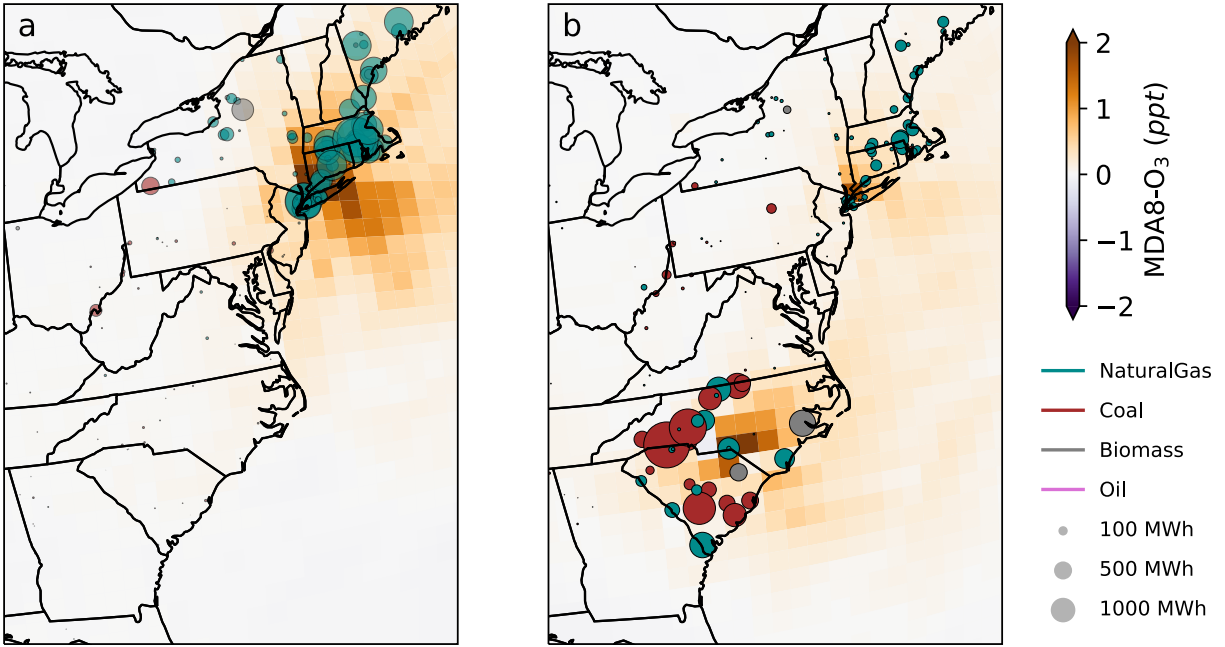


Figure S15: The electricity grid response and the induced seasonal average ground-level MDA8-O₃ (maximum daily 8-hour average) concentration for June, July and August (JJA) from electricity purchase by a) University A, and b) Corporate B

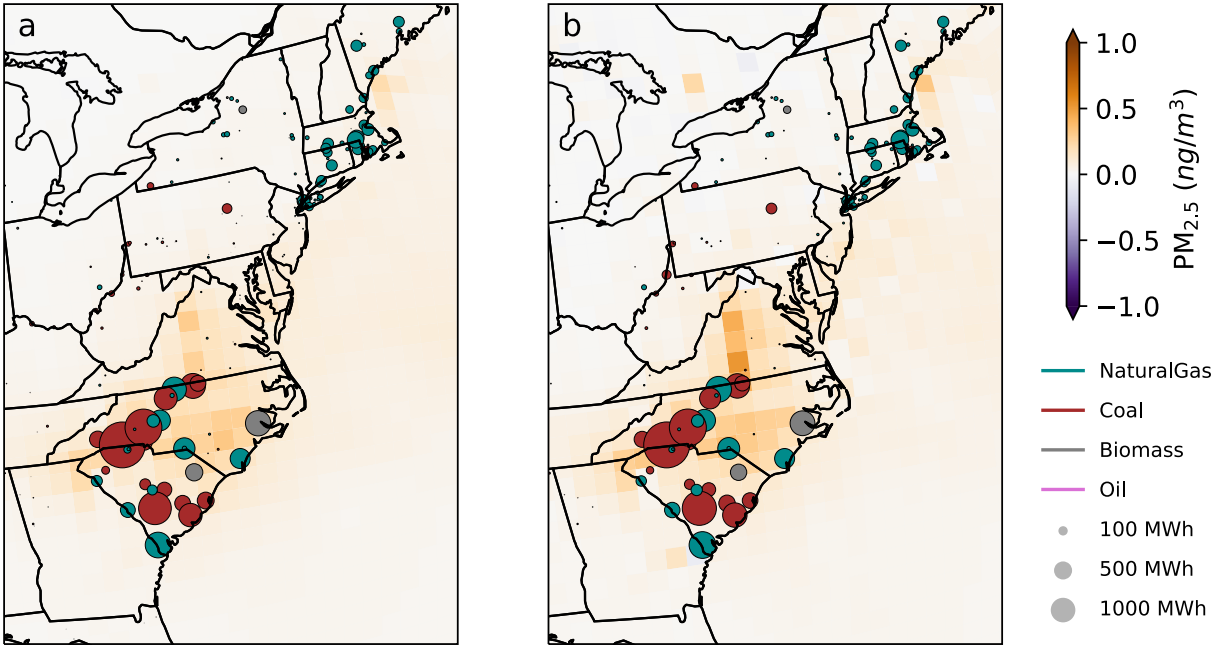


Figure S16: The energy generation and yearly-average ground-level PM_{2.5} concentration due to electricity purchase for test cases a) *Ten* (divided by ten for better comparison) and b) *Steady*

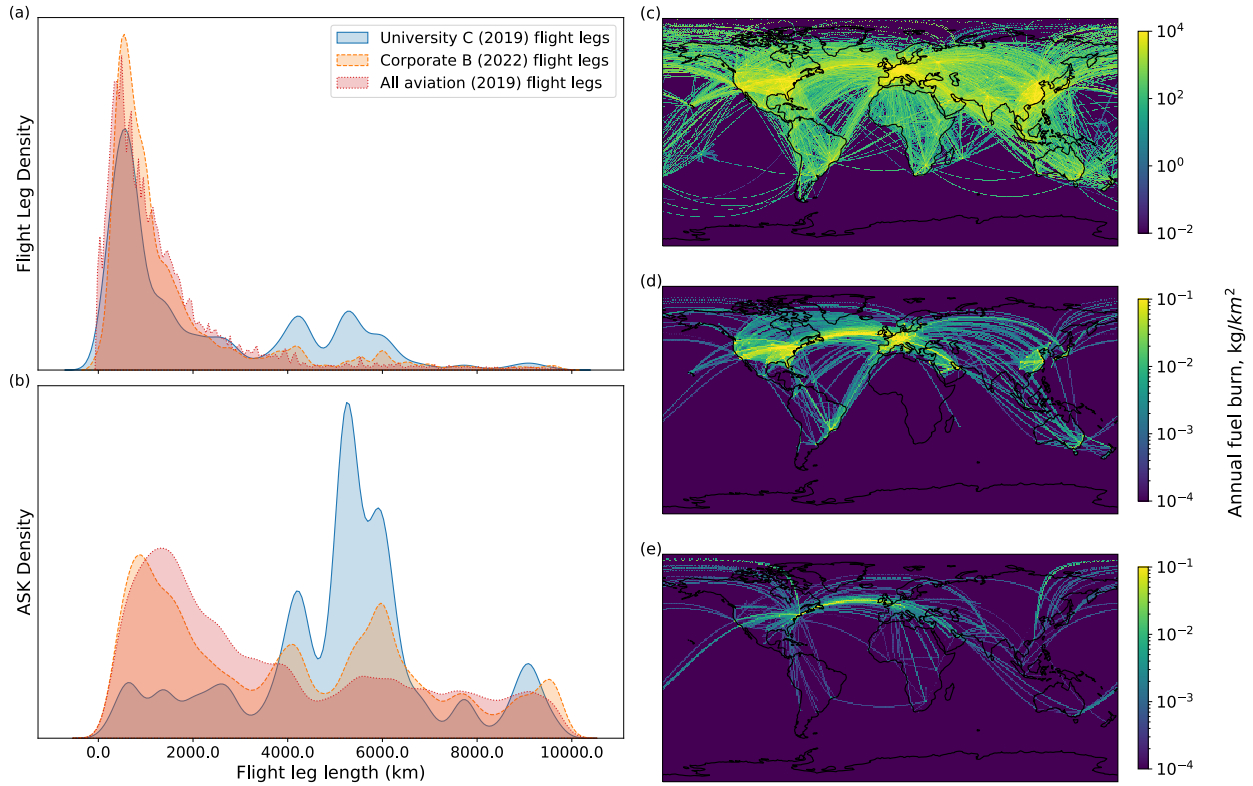


Figure S17: Distribution of number of flight legs (a) and available seat kilometer (ASK) (b) across different flight leg length intervals by global and organization air travel. Fuel burn spatial distribution caused by c) global air travel in 2019; d) Corporate B air travel in 2022; e) University C air travel in 2019. Kernel density estimation (KDE) was performed using a Gaussian kernel with a bandwidth adjustment of 0.5 for flight leg density and 0.2 for ASK density, providing a smoothed representation of the data distributions.

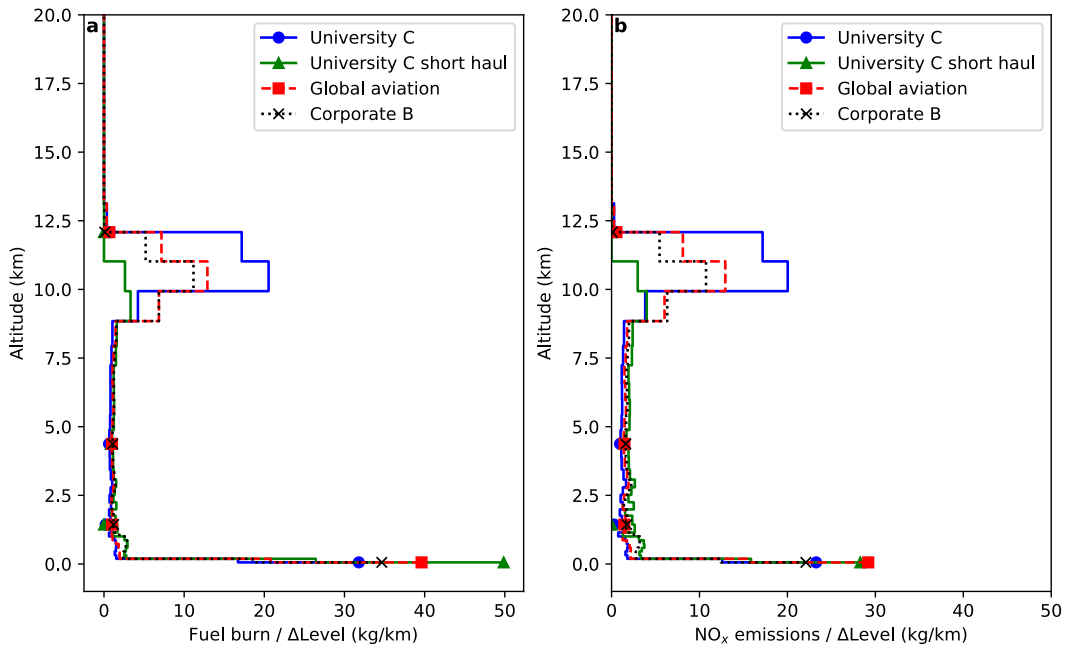


Figure S18: Fuel burn and NO_x emissions across altitude for different organizations

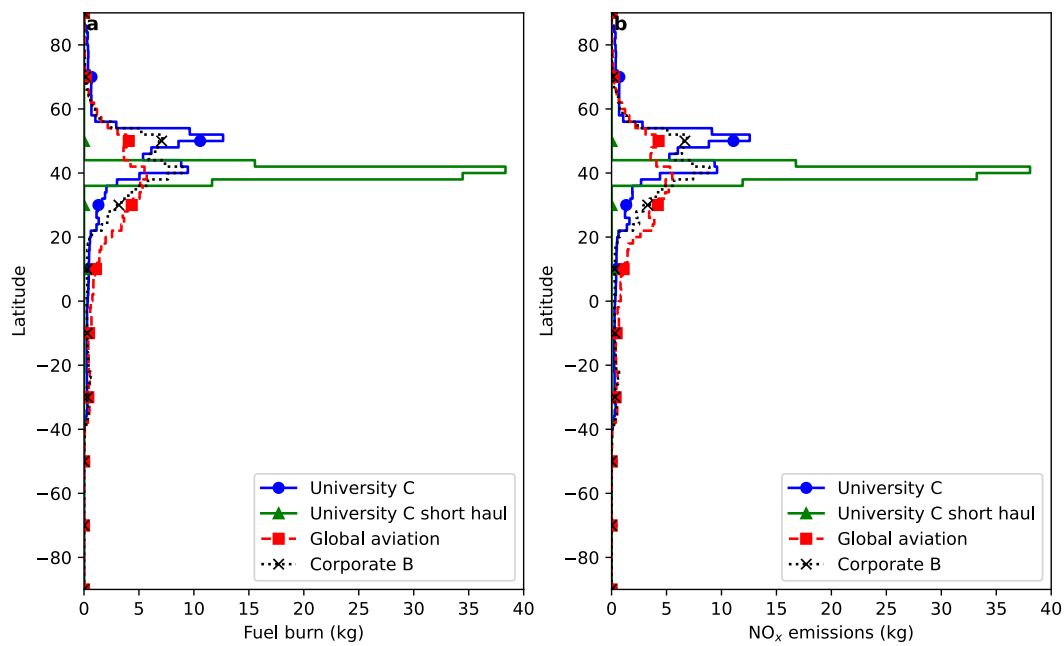


Figure S19: Fuel burn and NO_x emissions across latitude for different organizations

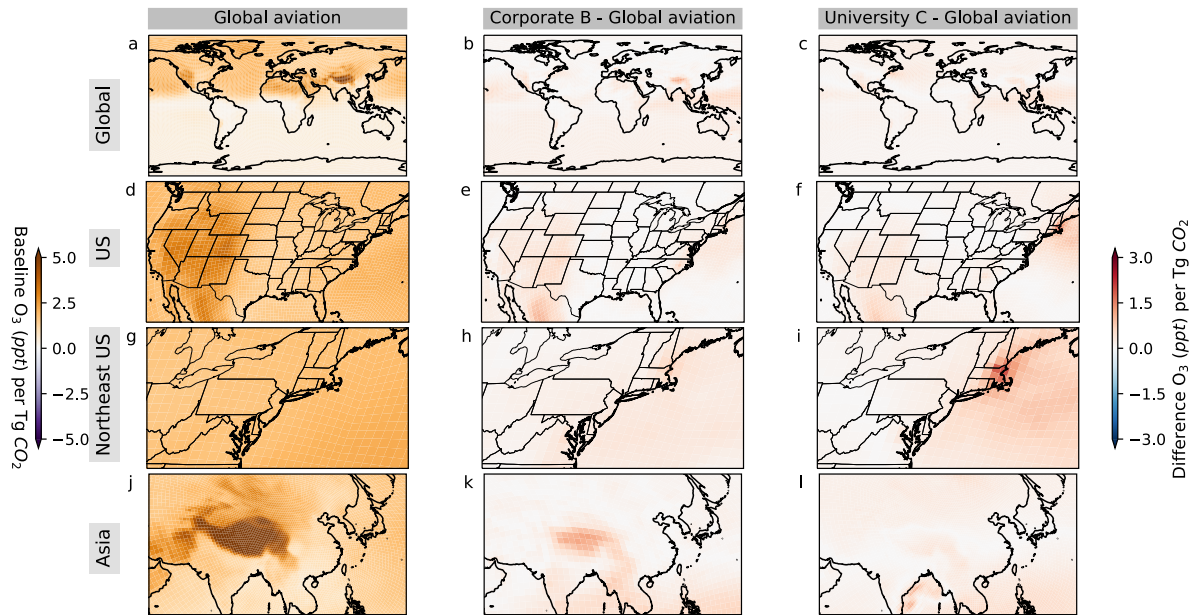


Figure S20: Ground-level changes in MDA8-O₃ concentration per teragram (Tg) of CO₂ emitted due to aviation activity. (a,d,g,j) show changes in PM_{2.5} concentration attributable to global aviation in 2019 (left axis). (b,e,h,k) show the difference in PM_{2.5} concentration between global aviation and Corporate B's air travel (right axis); (c,f,i,l) show the difference in PM_{2.5} concentration between global aviation and University C's air travel (right axis). Vertical stack shows different regions.

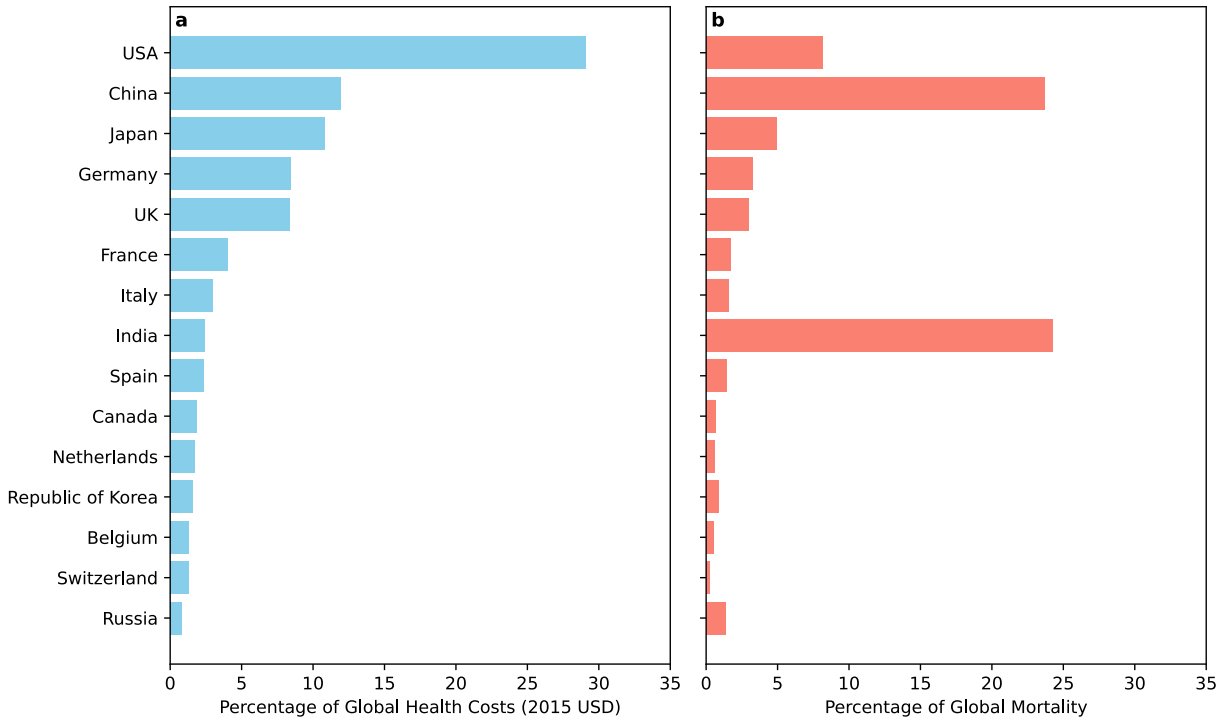


Figure S21: Top 15 countries with the highest air quality health costs from University C's 2019 air travel

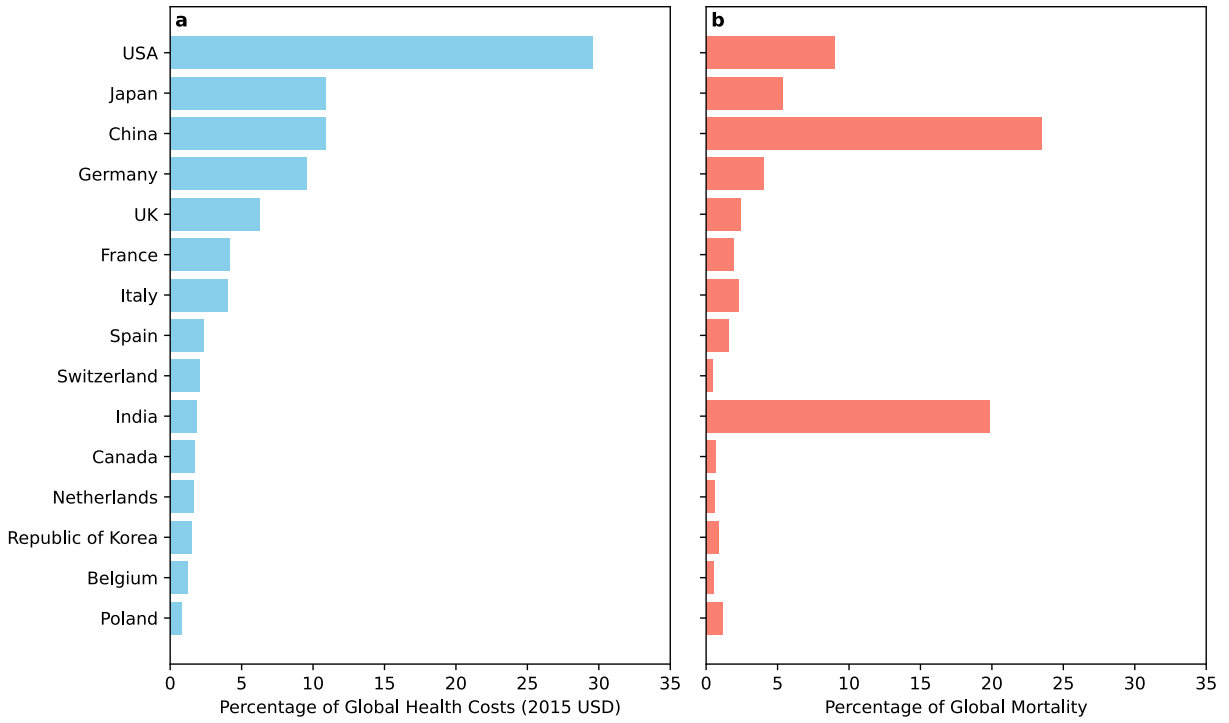


Figure S22: Top 15 countries with the highest air quality health costs from Corporate B's 2022 air travel

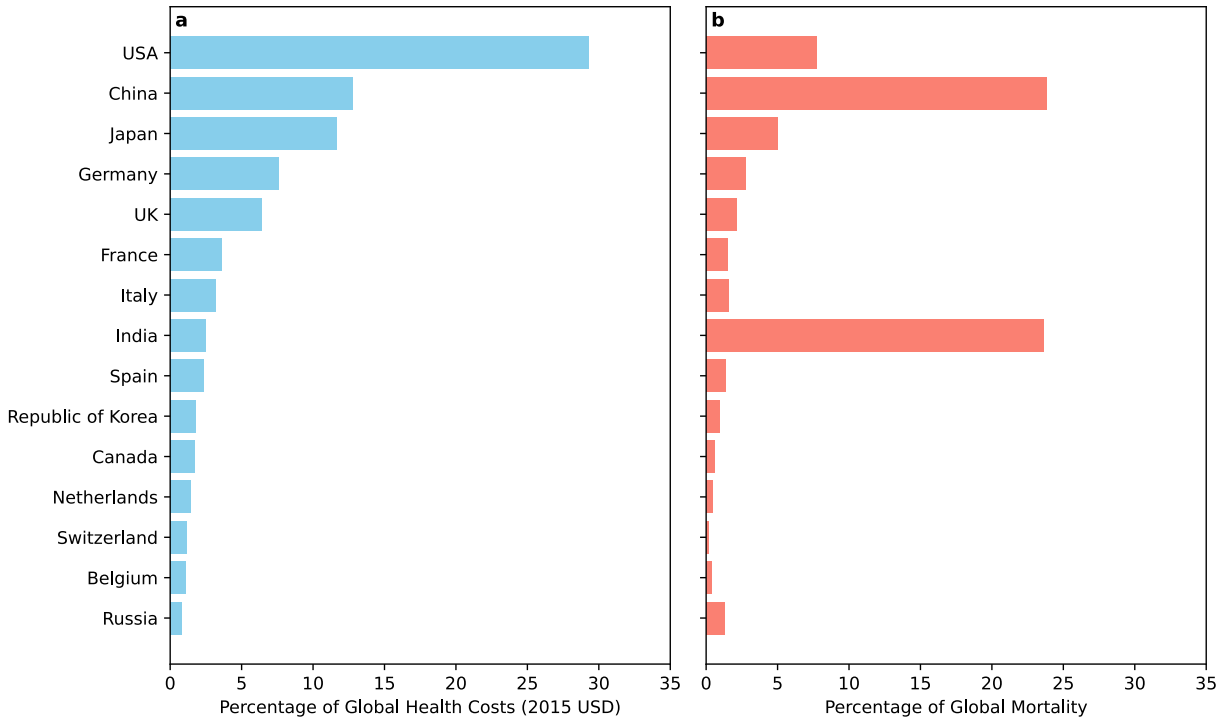


Figure S23: Top 15 countries with the highest air quality health costs from global aviation's 2019 air travel

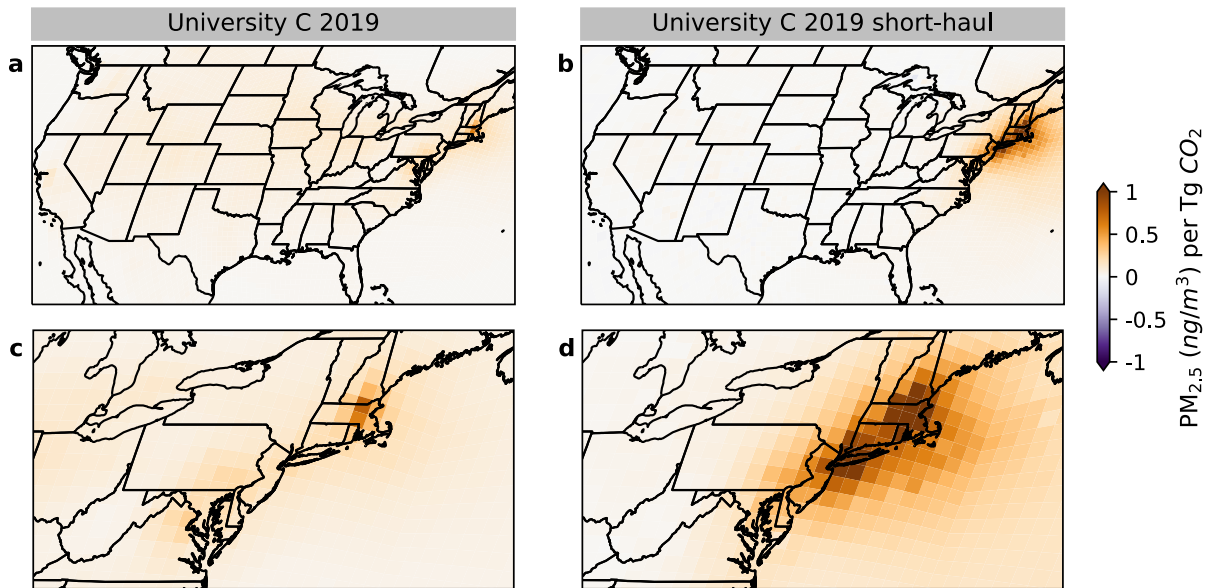


Figure S24: Ground-level changes in PM_{2.5} concentration (ng/m^3) per teragram (Tg) of CO₂ emitted due to (a), (c) University C's air travel in 2019 and (b), (d) University C's air travel with only short-haul flight legs in 2019. (a), (b) show the US results, and (c), (d) show results in the US Northeast.

SI References

- [1] US Environmental Protection Agency. Epa’s power sector modeling platform v6 using ipm summer 2021 reference case. <https://www.epa.gov/power-sector-modeling/epas-power-sector-modeling-platform-v6-using-ipm-summer-2021-reference-case>, 2021. Accessed: March 31, 2025.
- [2] Center for International Earth Science Information Network. Gridded population of the world, version 4 (gpwv4): National identifier grid, revision 11. <https://405sedac.ciesin.columbia.edu/data/set/gpw-v4-national-identifier-grid-406rev11>, 2017.
- [3] World Health Organization. Who methods and data sources for country-level causes of death 2000–2016. https://terrance.who.int/mediacentre/data/ghe/541healthinfo/Deaths/GHE2016_COD_methods.pdf, 2018.
- [4] R. Burnett, H. Chen, M. Szyszkowicz, N. Fann, B. Hubbell, III Pope, C. A., J. S. Apte, M. Brauer, A. Cohen, S. Weichenthal, J. Coggins, Q. Di, B. Brunekreef, J. Frostad, S. S. Lim, H. Kan, K. D. Walker, G. D. Thurston, R. B. Hayes, C. C. Lim, M. C. Turner, M. Jerrett, D. Krewski, S. M. Gapstur, W. R. Diver, B. Ostro, D. Goldberg, D. L. Crouse, R. V. Martin, P. Peters, L. Pinault, M. Tjepkema, A. van Donkelaar, P. J. Villeneuve, A. B. Miller, P. Yin, M. Zhou, L. Wang, N. A. H. Janssen, M. Marra, R. W. Atkinson, H. Tsang, T. Q. Thach, J. B. Cannon, R. T. Allen, J. E. Hart, F. Laden, G. Cesaroni, F. Forastiere, G. Weinmayr, A. Jaensch, G. Nagel, H. Concin, and J. V. Spadaro. Global estimates of mortality associated with long-term exposure to outdoor fine particulate matter. *Proc. Natl. Acad. Sci. U.S.A.*, 115(38):9592–9597, 2018.
- [5] M. C. Turner, M. Jerrett, III Pope, C. A., D. Krewski, S. M. Gapstur, W. R. Diver, B. S. Beckerman, J. D. Marshall, J. Su, D. L. Crouse, et al. Long-term ozone exposure and mortality in a large prospective study. *Am. J. Respir. Crit. Care Med.*, 193(10):1134–1142, 2016.
- [6] K. Rennert, F. Errickson, B. C. Prest, L. Rennels, R. G. Newell, W. Pizer, C. Kingdon, J. Wingenroth, R. Cooke, B. Parthum, D. Smith, K. Cromar, D. Diaz, F. C. Moore, U. K. Müller, R. J. Plevin, A. E. Raftery, H. Ševčíková, H. Sheets, J. H. Stock, T. Tan, M. Watson, T. E. Wong, and D. Anthoff. Comprehensive evidence implies a higher social cost of CO₂. *Nature*, 610(7933):687–692, 2022.
- [7] The International Council on Clean Transportation. Annual report of the international council on clean transportation in 2019. <https://theicct.org/sites/default/files/ICCT-AnnualReport-2019.pdf>, 2019.
- [8] R. Babikian, S. P. Lukachko, and I. A. Waitz. The historical fuel efficiency characteristics of regional aircraft from technological, operational, and cost perspectives. *J. Air Transp. Manag.*, 8(6):389–400, 2002.

- [9] C. Fountoukis and A. Nenes. Isorropia ii: A computationally efficient thermodynamic equilibrium model for K^+ - Ca^{2+} - Mg^{2+} - NH_4^+ - Na^+ - SO_4^{2-} - NO_3^- - Cl^- - H_2O aerosols. *Atmos. Chem. Phys.*, 7(17):4639–4659, 2007.
- [10] M. Qiu, Y. Weng, J. Cao, N. E. Selin, and V. J. Karplus. Improving evaluation of energy policies with multiple goals: Comparing ex ante and ex post approaches. *Environ. Sci. Technol.*, 54(24):15584–15593, 2020.
- [11] D. K. Henze, J. H. Seinfeld, and D. T. Shindell. Inverse modeling and mapping us air quality influences of inorganic $\text{pm}_{2.5}$ precursor emissions using the adjoint of geos-chem. *Atmos. Chem. Phys.*, 9(16):5877–5903, 2009.
- [12] M. Kopacz, D. J. Jacob, D. K. Henze, C. L. Heald, D. G. Streets, and Q. Zhang. Comparison of adjoint and analytical bayesian inversion methods for constraining asian sources of carbon monoxide using satellite (mopitt) measurements of co columns. *J. Geophys. Res. Atmos.*, 114(D4), 2009.